REPORT DOCUMENTATION PAGE

Form Approved
OMB No. 0704-0188

1. AGENCY USE ONLY (*Leave Blank*)	2. REPORT DATE	3. REPORT TYPE AND DATES COVERED
	10/25/95	Final Report

4. TITLE AND SUBTITLE
High Efficiency TiO_2 Photocatalysts by the Sol-gel Process

5. FUNDING NUMBERS
DAAH04-95-C-0028

6. AUTHOR(S)
Yuhong Huang
Cheng-Jye Chu

7. PERFORMING ORGANIZATION NAME(S) AND ADDRESS(ES)
CHEMAT TECHNOLOGY, INC.
19365 Business Center Dr. #8 & 9
Northridge, CA 91324

8. PERFORMING ORGANIZATION REPORT NUMBER
CTAR06

9. SPONSORING/MONITORING AGENCY NAME(S) AND ADDRESS(ES)
U.S. Army Research Office
P.O. Box 12211
Research Triangle Park, NC 27709-2211

10. SPONSORING/MONITORING AGENCY REPORT NUMBER
ARO 34492.1-CH-SAH

11. SUPPLEMENTARY NOTES
The view, opinions and/or findings contained in this report are those of the authors and should not be connstrued as an official Department of the Army position, policy, or decision, unless so designated by other documentation.

12a. DISTRIBUTION/AVAILABILITY STATEMENT
Approved for public release; distribution unlimited

12b. DISTRIBUTION CODE

13. ABSTRACT (*Maximum 200 words*)

The civilian, commercial, and defense sectors of most advanced industrialized nations are faced with a tremendous set of environmental problems related to the remediation of hazardous wastes, contaminated groundwaters, and the control of toxic air contaminations.

Semiconductor photocatalysis with a primary focus on TiO_2 as a durable and potential low-cost photocatalyst has been applied to a variety of problems of environmental interest. The efficiency of photochemical reactor for degradation of toxic and hazardous chemical substances is dependent on several factors: 1) Specific surface area, particle size and pore size of TiO_2 material, 2) Surface state and morphologies of TiO_2 material, 3) The crystallographic phase of TiO_2, 4) Doping effect, 5) Light harvestivity or dye-sensitization, 6) Translucency of photocatalyst, and 7) Kinetics of photoredox processes.

In Phase I work, the feasibility of both TiO_2 powder and film has been demonstrated. Efficiency of reactor using dye-sensitized and tungsten doped TiO_2 with high specific surface area has been improved by about 5 to 17 times compared to that of commercial Degussa P25 TiO_2 powder. Several technologies developed in Phase I project offers the opportunity for building a pilot scale unit .

14. SUBJECT TERMS	15. NUMBER OF PAGES
Photocatalysis, TiO_2, Sol-gel Process	45
	16. PRICE CODE

17. SECURITY CLASSIFICATION OF REPORT	18. SECURITY CLASSIFICATION OF THIS PAGE	19. SECURITY CLASSIFICATION OF ABSTRACT	20. LIMITATION OF ABSTRACT
Unclassified	UL	UL	UL

DISCLAIMER NOTICE

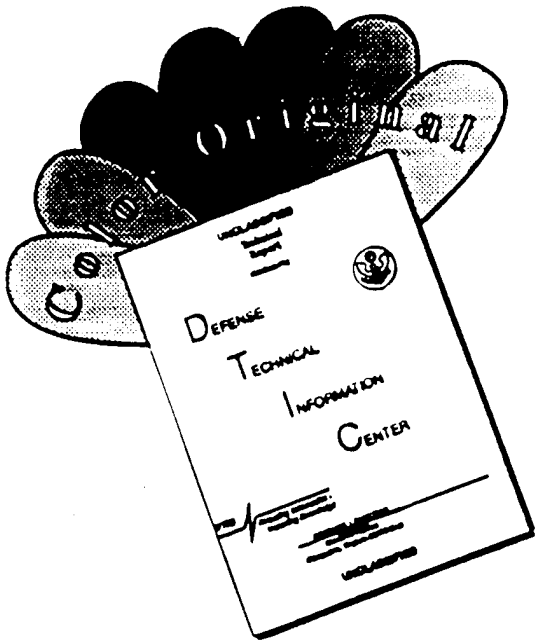

THIS DOCUMENT IS BEST QUALITY AVAILABLE. THE COPY FURNISHED TO DTIC CONTAINED A SIGNIFICANT NUMBER OF COLOR PAGES WHICH DO NOT REPRODUCE LEGIBLY ON BLACK AND WHITE MICROFICHE.

High Efficiency TiO_2 Photocatalysts by the Sol-Gel Precess

Authors:

Yuhong Huang

Cheng-Jye Chu

Final Report

April 1, 1995 - Sept. 30, 1995

Prepared for

Army

under

Contract No. DAAH04-95-C-0028

CHEMAT TECHNOLOGY, INC.

19365 Business Center Drive, #8 & 9

Northridge, CA 91324

October 15, 1995

High Efficiency TiO_2 Photocatalysts by the Sol-Gel Precess

Table of Contents

I. INTRODUCTION

The civilian, commercial, and defense sectors of most advanced industrialized nations are faced with a tremendous set of environmental problems related to the remediation of hazardous wastes, contaminated groundwaters, and the control of toxic air contaminations[1].

Problems with hazardous wastes at military installations are related in part to the disposal of chemical wastes in lagoons, underground storage tanks, and dump sites. As a consequence of these disposal practices, the surrounding soil and underlying groundwater aquifers have become contaminated with a variety of hazardous chemicals. The project cost for cleanup at more than 1800 military installations in the United States have been put at $30 billion; the time required for cleanup has been estimated to be more than 10 years.

In the civilian sector, the elimination of toxic and hazardous chemical substances such as the halogenated hydrocarbons from waste effluents and previously contaminated sites has become a major concern. More than 540 million metric tons of hazardous solid and liquid waste are generated annually by more than 14000 installations in the United States. A significant fraction of these wastes are disposed on the land each year. Some of these wastes eventually contaminate groundwater and surface water.

Semiconductor photocatalysis with a primary focus on TiO_2 as a durable and potential low-cost photocatalyst has been applied to a variety of problems of environmental interest. In addition to chemical waste treatment, it can also be useful for the destruction of microganisms such as bacteria and viruses, for the inactivation of cancer cells, for odor control, for the photosplitting of water to produce hydrogen gas, for the fixation of nitrogen, and for the clean up of oil spills.

Among a number of semiconductors that has been investigated, TiO_2 received the most attention for using both artificial and solar irradiation. However, because of the wide band gap at 3.2 ev , TiO_2 only collects light in the UV region. Therefore, only about 1% of the solar spectrum is utilized by TiO_2 photocatalysis, which is very inefficient outdoor. Several approaches have been undertaken to extend the absorption and conversion capacity of TiO_2 into the visible region of the solar spectrum. One approach is to dope TiO_2 with metal or metal oxide, such as Ag, Au, Pt, Pd, Ru, RuO_2, WO_3 and MoO_3 to increase the catalysts surface acidity[2], therefore increasing remarkably the photocatalytic activity.

Another approach is to sensitize TiO_2 by charge injection using dyes. A recent breakthrough by Grätzel et al. using a dye-sensitized TiO_2 colloidal film by the sol-gel process achieved a high absorption of the incident solar energy flux(46%) and showed a high proportion of the conversion of incident photons to electrical current (more than 80%)[3]. The overall light-to-electrical energy conversion yield is 7.1-7.9% in simulated solar light and 12% in diffuse daylight. The large current densities(greater than $12mAcm^{-2}$) and exceptional stability, as well as the low cost, make practical applications feasible[4]. However, no effort has been done on photocatalytic

activity of this dye-sensitized TiO_2.

In very fine particles, the diffusion of charge carries from the interior to the particle surface can occur more rapidly than their recombination. When the particle size decreases down to a 50 Å, quantum size effect should be taken into account. It is feasible to obtain quantum yields for photoredox processes approaching unity. Ahmed[5] used titania-silica (TiO_2-SiO_2) aerogels as photocatalysts to oxidize/degrade aqueous cyanide species. This aerogel photocatalysts were prepared by the sol-gel technique and supercritical drying. He has proven that the high translucent TiO_2-SiO_2 aerogel granules has higher efficiency in the photocatalytic oxidation of CN^- species compared to anatase TiO_2 powder.

The aim of Phase I project is focused on improvement of photocatalytic efficiency of elimination of hazardous chemical compounds from water using TiO_2 powder. Investigations were carried out to develop a technology of:

i) increasing the specific surface area and porosity of both TiO_2 powder and films,

ii) decreasing the particle size,

iii) obtaining anatase/rutile structure,

iv) investigation of the effects of surface morphology and surface defect.

Three sol-gel techniques were involved in Phase I project: 1) conventional sol-gel route; 2) aerosol, and 3) aerogel methods.

In Phase I work, the feasibility of fabricating a high efficient solar photochemical reactor by sol-gel route was successfully demonstrated. It was found that the efficiency of photochemical reactor for degradation of toxic and hazardous chemical substances is dependent on several factors: 1) Specific surface area, particle size and pore size of TiO_2 material, 2) Surface state and morphologies of TiO_2 material, 3) The crystallographic phase of TiO_2 , 4) Doping effect, 5) Light harvestivity or dye-sensitization, 6) Translucency of photocatalyst, and 7) Kinetics of photoredox processes. The approach to make high efficient reactor has been identified in Phase I program. Several times higher reactivity comparing to widely used Degussa P25 TiO_2 powder has been demonstrated in a short six-month effort.

In Phase I, TiO_2 photocatalyst in the forms of powders, granules, and films, has been prepared by conventional sol-gel route, aerosol, and aerogel process. Very high specific surface area of TiO_2 materials up to 460 m^2/g has been achieved in Phase I work. In this case, quantum effect should be taken into account. It is feasible to obtain quantum yields for photoredox processes approaching unity. High efficiency of photo-elimination of chemical waste can expected due to both high quantum yield and surface area. In Phase I project, it was found that reactivity of TiO_2 photocatalyst for treatment of 4-chlorophenol (ClC_6H_4OH, 4-CP) aqueous waste in solar irradiation improved 3 times by increasing surface area, 3.5 times by using dye-sensitized TiO_2, 2 times by adjusting anatase/rutile phases, 1.5 times by using tungsten doping and 1.5 times due to

different morphologies. By simply integrating these factors, high efficient TiO_2 photocatalyst can be expected.

The photo-elimitation of chemical waste is found also to depend on chemicals. Reactivity of degradation of dimethyl methyl phosphonate $\{CH_3P(O)(OCH_3)_2$, DMMP$\}$ using tungsten doped high surface area of TiO_2 is more than 20 times higher than that using Degussa P25 TiO_2. However, reactivity on 4-CP aqueous waste using same sample is only 5 times larger compared to that of Degussa P25 TiO_2 Powder. The effects is much higher in the case of DMMP. The possible reasons may be due to different surface area and using MeOH as a solvent, because oxidative electron transfer occurs exclusively through a surface-bound hydroxyl radical, $\{>TiOH^{\bullet}\}^{+}$ or equivalent trapped hole species. Degussa P25 powder is stoichiometric TiO_2. The TiOH radical might exist in the titanium oxide powder through sol-gel route thermal treated at low temperature. This may enhance the oxidation of chemical waste, especially in the case of non-aqueous solution.

The feasibility of both TiO_2 powders, granules, and films has been demonstrated. The combination of ormocer and aerogel (aero-ormocer) process has been proved to give the same TiO_2 materials with identical properties as that from aerogel process after annealing at high temperature, with better mechanical properties and can easier to make monolith materials. The photocatalysis effect of TiO_2-SiO_2 system prepared from titanium alkoxide and polydimethyl siloxane (PDMS) has also been proven.

As discussed above, the efficiency of photocatalytic reactor is controlled by seven parameters. High specific surface area of TiO_2 has been achieved in Phase I program. The crystallographic phase can controlled by change of annealing temperature. The morphology of TiO_2 can be modified by employing different techniques developed in Phase I work. The light harvestivity of TiO_2 photocatalyst is proven being improved by dye-sensitization. Tungsten doping effects as a function of W content has been investigated and proven.

Several technologies developed in Phase I project offers the opportunity for photocatalytic (use powder or film without counter electrode) and photoelectrochemical (use cell structure with counter electrode) applications of chemical waste treatment. The reactors of high efficiency with low cost and/or very high efficiency with moderate cost can be expected depending on the techniques employed.

In the following sections, technology of semiconductor photocatalysis for elimination of toxic and hazardous chemical substances are assessed. The recent exciting achievements in this company on degradation of chlorinated hydrocarbons such as 4-chlorophenol and dimethyl methyl phosphonate (DMMP) using TiO_2 powder with high specific surface area are summarized. Identification of work for Phase II program is described. The conclusions are presented.

II. OBJECTIVES

Objective of Phase I project is to demonstrate that the dye-sensitized and doped TiO_2 materials by sol-gel process can be used in the photocatalytic reaction for oxidation of chemical wastes under the simulated solar irradiation, and to develop innovative technologies to improve the efficiency of photodegradation of chemical waste. In Phase I research, we met the following goals:

1. Development of various technologies on fabrication of TiO_2 materials including powders, films and porous aerogels with much higher specific surface area comparing to commercial TiO_2 anatase powder- Degussa P25 powder.
2. Characterization of crystallographic phase development, morphologies and surface area of TiO_2 materials using XRD, SEM and BET analyser.
3. Investigation on effects of various parameters, such as tungsten doping, dye-sensitization, crystallographic phase, morphologies and specific surface area, on efficiency of photodegradation of chemical waste under the simulated solar radiation.
4. Improvements of photocatalytic efficiency by developing innovative technologies, such as TiO_2 using aerosol and aerogel routes with doping and sensitized dye.

The aim of our work is focused on improvement of photocatalystic efficiency through the four routes as discussed above. The sol-gel technology for TiO_2 powder and film is chosen because of a variety of advantages, including low processing temperature, the possibility of achieving large specific surface area, and simple and inexpensive equipment. Hydrolysis of Ti alkoxide can result in very fine network structure with low density. The large specific surface area can be obtained by following suitable drying and sintering process.

III. BACKGROUND

3.1 Mechanisms of Semiconductor Photocatalysis

Semiconductor TiO_2 can act as sensitizers for light-reduced redox processes due to its electronic structure, which is characterized by a filled valence band and an empty conduction band. When a photon with an energy of hv matches or exceeds the bandgap energy, E_g, of the TiO_2 , an electron, e_{cb}^-, is promoted from the valence band, VB, into the conduction band, CB, leaving a hole, h_{vb}^+ behind (see Figure 3.1). Excited-state conduction-band electrons and valence-band holes can recombine and dissipate the input energy as heat, get trapped in metastable surface states, or react with electron donors and electron acceptors adsorbed on the semiconductor surface or within the surrounding electrical double layer of the charged particles.

In the absence of suitable electron and hole scavengers, the stored energy is dissipated within a few nanoseconds by recombination. If a suitable scavenger or surface defect state is available to trap the electron or hole, recombination is prevented and subsequent redox reactions may occur. The valence-band holes are powerful oxidants (+1.0 to +3.5 V vs NHE depending on the semiconductor and pH), while the conduction-band electrons are good reductants (+0.0 to -1.5 V vs NHE). Most organic photodegradation reactions utilize the oxidizing power of the holes either directly or indirectly; however, to prevent a buildup of charge one must also provide a reducible species to react with the electrons. In this general mechanism, it is assumed that oxidative electron transfer occurs exclusively through a surface-bound hydroxyl radical, $\{>TiOH^{\bullet}\}^+$ or equivalent trapped hole species.

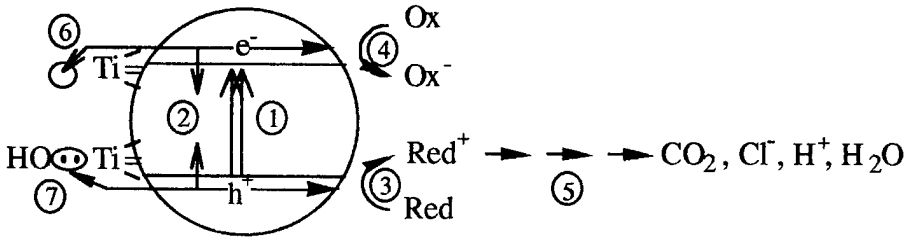

Figure 3.1 Primary steps in the photoelectrochemical mechanism. (1) formation of charge carriers by a photon; (2) charge carrier recombination to liberate heat; (3) initiation of an oxidative pathway by a valence-band electron; (5) further thermal (e.g., hydrolysis or reaction with active oxygen species) and photocatalytic reactions to yield mineralization products; (6) trapping of a conduction-band electron in a dangling surficial bond to yield Ti(III); (7) trapping of a valence-band hole at a surficial titanol group.

A general stoichiometry for the heterogeneously photocatalyzed oxidation of a generic chlorinated hydrocarbon to complete mineralization can be written as follows:

$$C_xH_yCl_z + (x + \frac{y-z}{4})\, O_2 \xrightarrow{h\nu\ TiO_2} x\, CO_2 + z\, H^+ + z\, Cl^- + (\frac{y-z}{2})\, H_2O \qquad (1)$$

On bulk semiconductor electrodes only one species, either the hole or electron, is available for reaction due to band bending. However, in very small semiconductor particle suspensions both species are present on the surface. Therefore, careful consideration of both the oxidative and the reductive paths is required.

The depletion layer at the interface between a bulk semiconductor and a liquid medium, plays an important role in light-induced charge separation. The local electrostatic field present in the space charge layer serves to separate the electron-hole pairs generated by illumination of the semiconductor. In the case of colloidal semiconductors, the band bending is small and charge separation occurs via diffusion. The absorption of light leads to the generation of electron-hole pairs in the particle which are oriented in a spatially random fashion along the optical path. These charge carriers subsequently recombine or diffuse to the surface where they undergo chemical reactions. For colloidal TiO_2 (D_e=2 × $10^{-2}cm^2/s$) with a radius of 6 nm the average transit time of the electron is 3ps based on Random Walk Model.[6] It should be noted that the random walk model breaks down for particles exhibiting quantum size effects. Here, the wave function of the charge carrier spreads over the whole semiconductor cluster and they do not have to undergo diffusional displacement to accomplish reactions with species present at the surface. Since in colloidal semiconductors, the diffusion of charge carriers from the interior to the particle surface can occur more rapidly than their recombination, it is feasible to obtain quantum yields for photoredox processes approaching unity.

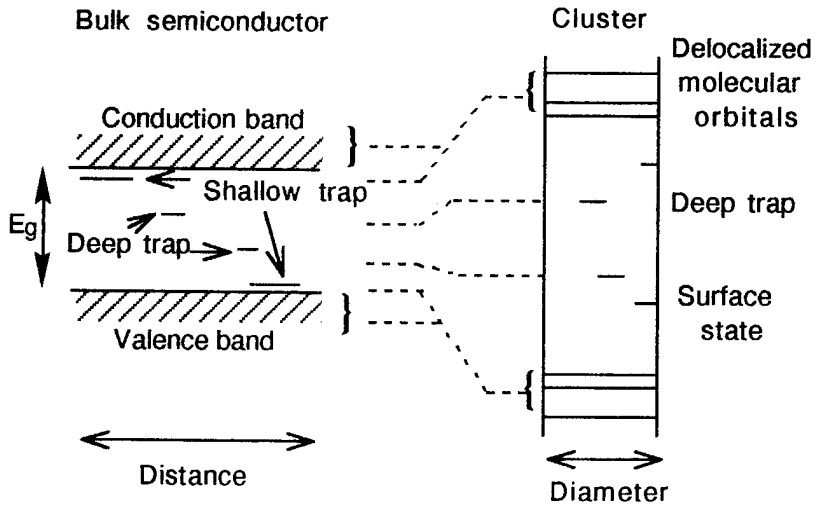

Figure 3.2. Spatial electronic state correlation diagram for bulk semiconductors and clusters.[7]

Quantum size effects are expected to occur when the Bohr radius of the first exciton in the

semiconductor becomes commensurate with or larger than that of the particle. A blue shift in the absorption and luminescence emission of small CdS particles was observed when their radius decreased below the size where charge carrier confinement effects should become noticeable. Apart from increasing the effective band gap, the effect of local confinement of the charge carriers is to produce discrete electronic states in the valence and conduction bands. A schematic illustration of these confinement effects is given in Figure 3.2.

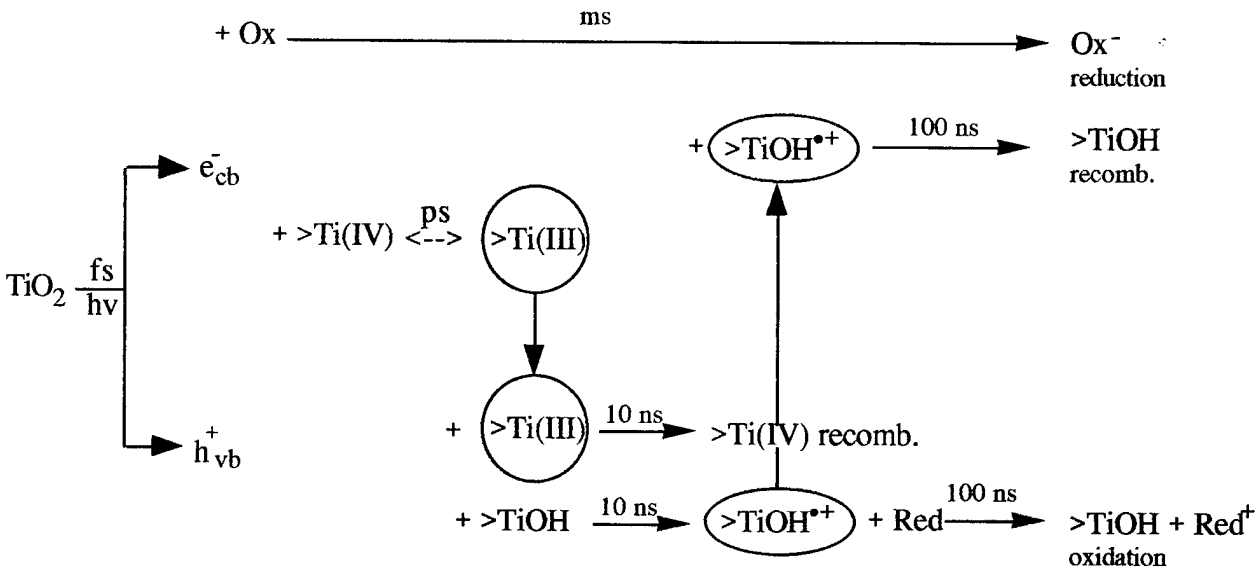

Figure 3.3. Kinetics of the primary steps in photoelectrochemical mechanism. Recombination is mediated primarily by >Ti(III) in the first 10 ns. Valence-band boles are sequestered as long-lived >TiOH$^{\cdot+}$ after10 ns. >TiOH is reformed by recombination with conduction-band electrons or oxidation of the substrate on the time scale of 100 ns.

Hoffmann[8] has proposed the general mechanism for heterogeneous photocatalysis on TiO_2. Characteristic times for the various steps in the mechanism are shown in Figure 3.3. >TiOH represents the primary hydrated surface functionality of TiO_2, e_{cb}^- is a conduction-band electron, e_{tr}^- is a trapped conduction-band electron, h_{vb}^+ is a valence-band hole, Red is an electron donor (i.e., reductant), Ox is an electron acceptor (i.e., oxidant), >TiOH$^{\cdot+}$ is the surface-trapped VB hole (i.e., surface-bound hydroxyl radical) and >TiOH is the surface-trapped CB electron. The overall quantum efficiency for interfacial charge transfer is determined by two critical processes. They are the competition between charge-carrier recombination and trapping (picoseconds to nanoseconds) followed by the competition between trapped carrier recombination and interfacial charge transfer (microseconds to milliseconds). An increase in either the

recombination lifetime of charge carriers or the interfacial electron-transfer rate constant is expected to result in higher quantum efficiencies for steady-state photolyses.

The efficiency of semiconductor photocatalysis depends on several factors including: i) large interfacial surface area; ii) fast interfacial electrontransfer rate constant; and iii) slow recombination and iv) increasing harvestivity of sunlight.[9] Bickley et al.[10] have suggested that the anatase/rutile structure of TiO_2 promote charge-pair separation and inhabits recombination. In very fine particles, the diffusion of charge carries from the interior to the particle surface can occur more rapidly than their recombination, therefore it is feasible to obtain quantum yields for photoredox processes approaching unity. Dye-sensitized nanocrystalline TiO_2 has shown very high efficiency due to both increasing the harvestivity of the sunlight and as a charge separation medium.

3.2. Doping of TiO_2 photocatalyst

There has been a number of attempts to improve the performance of TiO_2 as a photocatalyst under UV illumination and to extend its light absorption and conversion capacity into the visible portion of the solar spectrum. In between these approaches, doping of TiO_2 with noble metal or metal oxide shows promising results.

Previously, photochemical deposition of metal on semiconductor particles has been used as a means of noble metal recovery in waste solutions. Recently, this technique has been widely employed for the purpose of improvement of photocatalytic activity of semiconductors. Pt, Pd, Au, Rh, RuO_2, etc., have been utilized in the improvement of photocatalytic activity. Several studies have shown that gold can be photodecomposed from aqueous solutions of $AuCl_3$ and the resulting photocatalyst has activities 30% higher than powders and films without the gold deposits[11]. Since the reduction of oxygen accompanying the photooxidation of organic compounds is the rate-determining step, a fast oxygen reduction rate is necessary for achieving a high quantum efficiency in the photoassisted oxidation of organic compounds. This can be achieved when catalytic sites are incorporated in the TiO_2 surface.

Both TiO_2 powders and films were used for the photocatalyst. Unlike the TiO_2 powders, TiO_2 films can be used repeatedly for the measurement of photocatalytic activity, and unlike highly dispersed powders, films present no problem in terms of separating the catalyst from the solution after degradation of the organic impurities. TiO_2 films on pyrex glass substrates were prepared and evaluated as photocatalysts. TiO_2 films can be prepared by nebulizing of dipropoxytitanium bis(acetylacetonate) solution. Figure 3.4 shows the change in the concentration of salicylic acid as a function of irradiation time using TiO_2 film as the photocatalyst[12]. The photodecomposition of the salicylic acid on TiO_2 films follows first-order kinetics. The slope in Figure 3.4, i.e., the rate of degradation of salicylic acid, was taken as the parameter for the evaluation of the photocatalytic activity of TiO_2 films. AgF was reduced onto the TiO_2 films on pyrex glass substrates by

photochemical decomposition. The film containing metallic silver particles shows higher photocatalytic activity. Other noble metal particles, e.g., Pd, Au also show similar effect. Papp et. al. have shown that adding palladium to TiO_2 increases its photocatalytic activity toward the degradation of DCB[13]. The addition of palladium to a TiO_2 film also increases the photocatalytic activity toward the degradation of salicylic acid. The metal particles are undoubtedly playing an important role in the transfer of electrons to the oxygen at the surface of the catalysts.

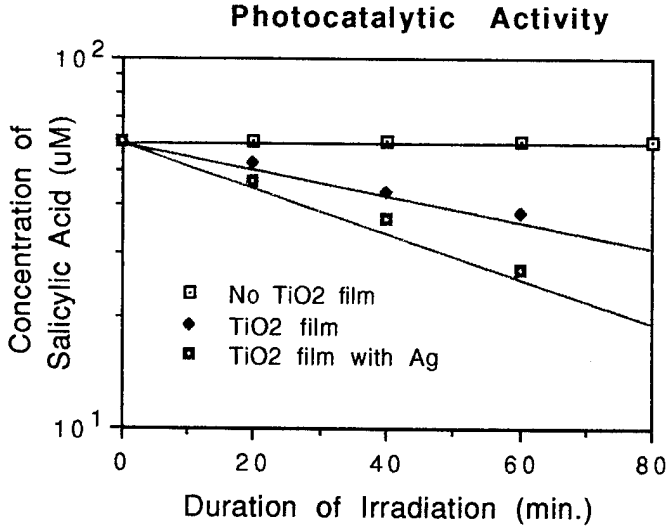

Figure. 3.4 Change in the concentration of salicylic acid as a function of irradiation time using TiO_2 film as the photocatalyst.

The other way to get higher efficiency is by using WO_3/TiO_2 and MoO_3/TiO_2 mixed oxide powders as the photocatalysts. The addition of WO_3 or MoO_3 to TiO_2 greatly enhanced its photocatalytic properties[14]. Figure 3.5 and Figure 3.6 show the decomposition of 1-4 dichlorobenzene and the surface acidity followed by the mole percents of WO_3 and MoO_3 impregnated on TiO_2 powders. The concentrations of WO_3 and MoO_3 which gave maximum photocatalytic activity were 3 and 2.5 mol%, respectively. These concentrations also gave maximum surface acidities. It appears that surface acidity plays an important role in determining the activity of the photocatalyst.

Photocatalytic activity of TiO_2 is influenced by surface area, crystal structure and density of surface hydroxyl groups. It has been suggested that TiO_2 (anatase) has a higher adsorptive activity for O_2 or H_2O and a stronger catalytic action than TiO_2 (rutile), probably due to the defective crystal structure of the anatase phase. Since TiO_2(anatase) is considered to be a thermodynamically metastable phase, a single crystal or sintered body of TiO_2 of anatase phase cannot be obtained by conventional preparation methods. Yoko et al. prepared TiO_2 film semiconductor electrode for photocleavage of water by the sol-gel process[15]. The sol-gel method combined with dip-coating technique have been used to prepare thin TiO_2 films on glass substrates. One of the advantages of

the sol-gel process is the thermodynamically metastable phase, in this case TiO_2 with anatase phase, may be obtained. This method of preparing TiO_2 films on the substrates also has many other advantages over other methods since (1) no special apparatuses are required, (2) uniform multicomponent films can easily be formed, (3) the resultant film may possibly be characterized by a porous structure with a large specific surface area. Sol-gel derived TiO_2 films were anatase on heating below 800°C and transformed into rutile.

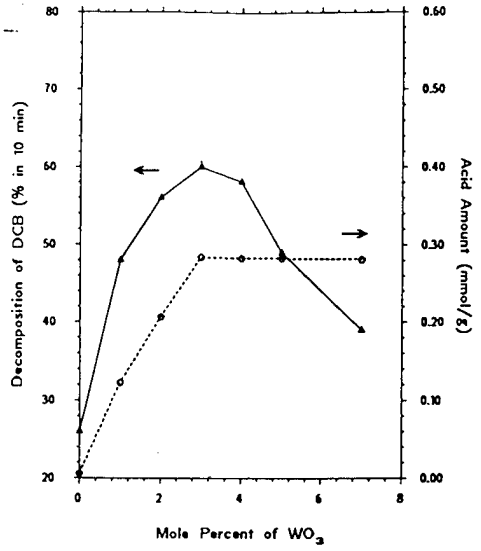

Figure. 3.5 Decomposition of DCB and the surface acidity followed by the mole percents of WO_3 impregnated on TiO_2 powders

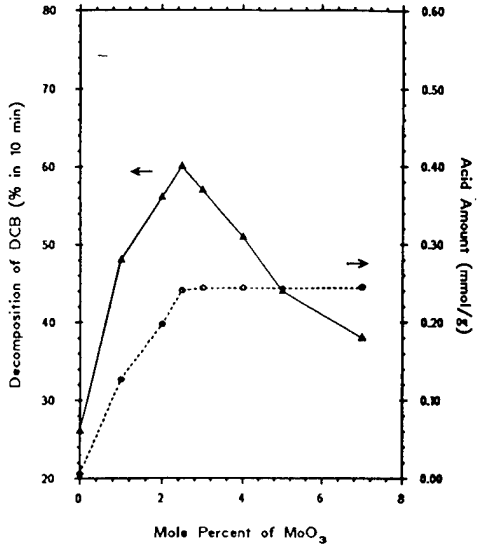

Figure. 3.6 Decomposition of DCB and the surface acidity followed by the mole percents of MoO_3 impregnated on TiO_2 powders

3.3. Dye-Sensitization of TiO_2

Another alternative way to fabricate photocatalytic cells with light absorption in the visible and the infrared region, and still benefit from the good stability of the large band gap semiconductors, is to make use of dye-sensitization. The dye-sensitization of semi-conducting electrodes was extensively investigated during the late sixties and the seventies, but the concept was abandoned and regarded as useless for photocatalyst applications. The two main reasons for the rejection of the concept were: (1) dyes in general were regarded not stable enough to meet the demands of the lifetime for an economically cells, and (2) the amount of dye adsorbed on the semiconductor was too low to give a sufficient absorption of light for a good efficiency. On a smooth surface, a monomolecular layer of sensitizer absorbs less than 1% of incident monochromatic light. Attempts to harvest more light by using multilayers of dye or increasing the roughness of the semiconductor surface have in general been unsuccessful, due to the lack of

photoactivity and the filtering effect of the dye molecules which are not in direct contact with the semiconductor.

A recent unexpected breakthrough is the discovery that TiO_2 films with a specific fractal-type surface texture can be sensitized with strikingly high yields. Grätzel et al. introduced the microporous colloidal TiO_2 film electrode by the sol-gel process as a supporting semiconductor for the dye. The TiO_2 particles (Figure 3.7) were prepared by hydrolysis of titanium tetraisopropoxide followed by autoclaving for 12 hour at 200°C[16]. Carbowax M-20,000 was added into the sol to form a viscous dispersion and spread on the conducting glass support and heated under air at

Figure. 3.7 Transmission electron micrograph of TiO_2 particles used in thin film production. The scale bar represents 10 nm.

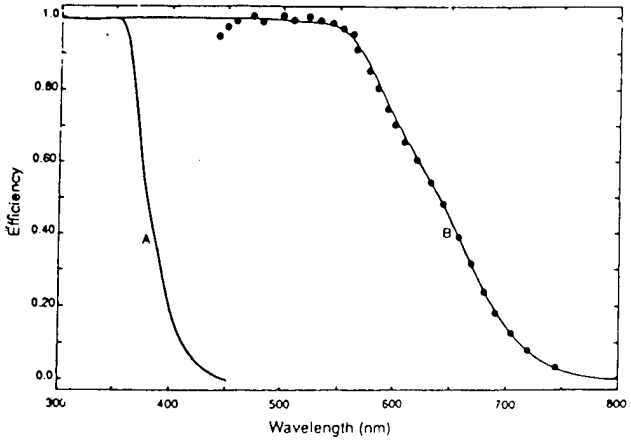

Figure. 3.8 shows the absorption spectra of such nanostructure TiO_2 films.

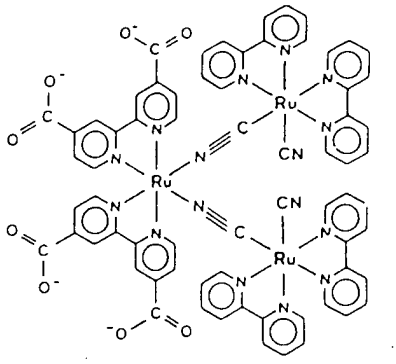

Figure. 3.9 Structure of $RuL_2(m\text{-}(CN)Ru(CN)L_2')_2$.

450°C for 30 min to produce electronic contact between particles. The device is based on a 10-μm-thick, optically transparent film of TiO_2 particles a few nm in size, coated with a layer of a charge-

transfer dye to sensitize the film for light harvesting. Because of the high surface area of the semiconductor film and the ideal spectral characteristics of the dye, the device harvests a high proportion of the incident solar energy flux(46%) and shows exceptionally high efficiencies for the conversion of incident photons to electrical current (more than 80%).

Figure 3.8 shows the absorption spectra of such nanostructure TiO_2 films. Curve A is the bare TiO_2 film displaying the fundamental absorption edge of anatase (band gap 3.2 ev) in the ultraviolet region. Deposition of a monolayer of the trimeric ruthenium complex, $RuL_2(\mu\text{-}(CN)Ru(CN)L_2')_2$, where L is 2,2' bipyridine-4,4'-dicarboxylic acid and L' is 2,2'-bipyridine (Figure 3.9), results in deep brownish-red coloration of the film. The absorption onset is shifted to 750 nm (curve B in Figure 3.8), the light harvesting efficiency reading almost 100% in the whole visible region below 550 nm. The two carboxylic functions on the 2,2'-bipyridine ligand L serve as interlocking groups through which the dye is attacted at the surface of TiO_2 films having a specific surface texture. The role of these interlocking groups is to provide strong electronic coupling between the π^* orbital of the 2,2'-bipyridine and the 3d-wave-function manifold of the conduction band of the TiO_2., allowing the charge injection to proceed at quantum yields close to 100%. The efficiency of the device at 1000W, AM1.5 solar simulator light is about 7.1-7.9 %, and in diffuse light (natural light) is about 12%. This is much higher than the normal TiO_2 film or powder electrode. Exceptional stability have also been demonstrated by sustaining at least five million turnovers without decomposition. This dye-sensitized TiO_2 films has by far been used on the solar energy conversion, no study has been done on the photocatalytic reactions for decomposition of waste chemicals.

A schematic drawing of the energy levels of a dye-sensitized nanocrystalline TiO_2 in contact with an electrolyte is shown in Figure 3.10. The desired pathway for a photoexcited electron is also indicated. Dye-sensitized TiO_2 differ from the conventional semiconductor is that they separate the function of light absorption from charge carrier transport. Promising results have so far been obtained with ruthenium complexes where at least one of the ligands was 4,4'-dicarboxy-2,2'-bipyridyl (Figure 3.10).

The two carboxylate groups serve to attach the Ru complex to the surface of the TiO_2 and to establish good electronic coupling between the π^* orbital of the electronically excited complex and the 3d wave function manifold of the TiO_2. The substitution of the bipyridyl with the carboxylate groups also lowers the energy of the π^* orbital of the ligand. Since the electronic transition in the dye is of metal to ligand charge transfer (MLCT) character, the excitation energy is channeled into the right ligand, i.e. the one from which electron injection into the conduction band takes place.

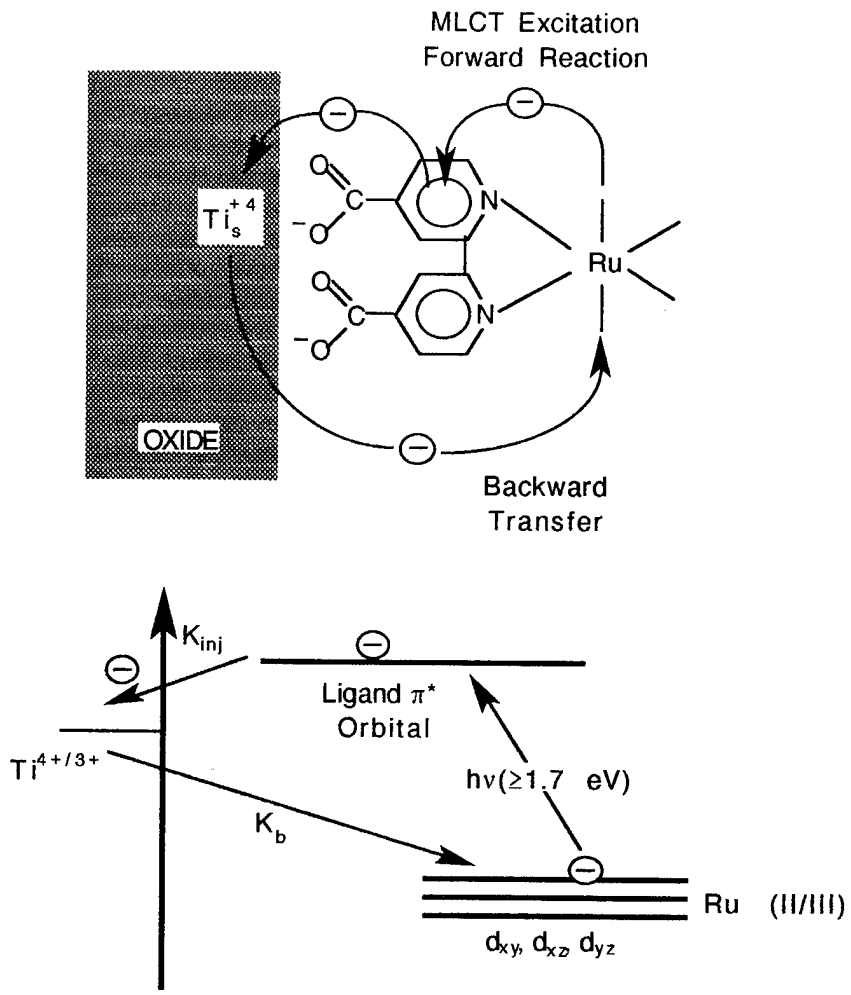

Figure 3.10. Photoinduced charge separation on the surface of titanium oxide. A ruthenium bipyridyl complex is used as a sensizer. Optical excitation involves electron transfer from the metal to the ligand (MLCT) followed by the interfacial charge injection into the titanium dioxide conduction band. The carboxylates function as interlocking groups attaching the complex to the surface of the oxide and enhancing electronic coupling with the solid. K_{inj} and K_b represent the rate constants for electron injection and recombination, respectively.

Similar effects have been observed with a number of different sensitizers such as porphyrines[17] and $Fe(CN)_6^{4-}$ surface derivatized TiO_2 particles[18]. In all these cases the back-electron transfer from the semiconductor particle to the oxidized sensitizer occurred with a rate that was several orders of magnitude slower than the forward injection. Thus, the combination of sensitizer with a colloidal semiconductor particle affords a molecular device for light-induced charge separation.

The dyes discussed in this section have two functions: 1) Absorption of visible light and transfer of charge to TiO_2 semiconductor; 2) serve as charge separation media. The high solar

energy conversion of this dye-sensitized TiO_2 should also confirm the possible high photocatalytic efficiency of this material in visible region.

3.4 Chemistry of the Sol-Gel Process

The sol-gel technique offers a low-temperature method for synthesizing ceramic materials which are either totally inorganic in nature or composed of inorganic and organics. The process is based on hydrolysis and condensation reaction of organometallic compounds in alcoholic solutions. Up to now, the sol-gel technique has been commercially used to fabricate ceramic powders (e.g. 3M's abrasive powders), fibers (e.g. Asahi's silica fiber), coatings and monolithic optical elements. Figure 3.11 shows an artistic drawing of the sol-gel process and the products.

The sol-gel process uses inorganic or metal organic precursors. The most commonly used organic precursors for sol-gel processing are metal alkoxides ($M(OR)_z$), where M stands for metal atom and the R represents a proton or other ligand like an alkyl group (C_xH_{2x+1}). Metal alkoxides are popular because they hydrolyzed readily with water under acidic, neutral or basic conditions, as in the following reaction :

$$Si(OR)_4 + H_2O \text{ --> } HO\text{-}Si(OR)_3 + ROH$$

Depending on the amount of water and catalyst present, hydrolysis may go to completion or stop while the metal is only partially hydrolyzed, $Si(OR)_{4-n}(OH)_n$. Two partially hydrolyzed molecules can link together in a condensation reaction, such as :

$$(OR)_3Si\text{-}OH + HO\text{-}Si(OR)_3 \text{ --> } (OR)_3Si\text{-}O\text{-}Si(OR)_3 + H_2O$$

or $$(OR)_3Si\text{-}OR + HO\text{-}Si(OR)_3 \text{ --> } (OR)_3Si\text{-}O\text{-}Si(OR)_3.+.\ ROH$$

Condensation reactions can continue to produce polymers with M-O-M bonds. After pyrolysis, an amorphous or crystalline ceramic can be produced by the sol-gel processing. Metal alkoxides can not only react with water but also with organic acids, such as acetylacetonate and alcohol amine, to reduce both their effective functionality and the rates of hydrolysis of condensation. By controlling the concentration of the chelating agents, the inorganic polymers formed after hydrolysis and polycondensation vary from linear or branched to two dimensional or three dimensional network. These chelating agents remain inside the network even after polycondensation.

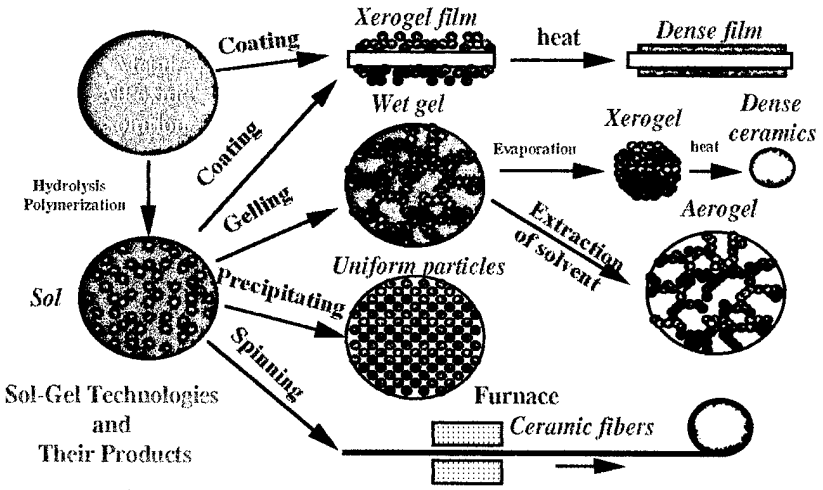

Figure 3.11. The schematic of sol-gel technologies and their products.

3.5. Advantages of the sol-gel process

The sol-gel process provides many advantages compare to other ceramic processing techniques. Which are: **(1) Low temperature processing:** Most of the sol-gel derived ceramic can be crystalized or densified at much lower temperatures than the traditional ceramic sintering processes. **(2) Adjustable chemical composition:** It is easier to mix or dope the materials in the sol-gel process by simply mixing or doping the precursors by the chemical route. Molecular level mixing is also possible, that can create materials with properties that traditional process can not achieved. **(3) Tailorable microstructure:** The microstructure of the materials in the sol-gel process is easier to control by the process parameters, while the microstructure of final materials are almost fixed in traditional ceramic process. **(4) Less limitation of size and shape:** Sol-gel process can be used to prepare powders, monoliths, fibers and films with large variety of size. Especially in film deposition, due to the high vacuum and cavity size limitations, large size and irregular shape deposition become expensive or even impossible for vapor routes, while in the sol-gel process these can actually been done in low cost. **(5) Low capital cost:** The vacuum and cavity systems in vapor deposition are expensive and the maintenance cost are high, while in the sol-gel process, the controlled atmosphere box and furnace are much cheaper and easier to maintain; **(6) Low operational cost and high productivity:** Especially in film process, the procedure in the sol-gel process is much simpler than the vapor deposition, therefore the operation cost for the sol-gel process is expected to be low, the productivity is also higher than the vapor routes.

3.6. Organically modified ceramics(ORMOCERS)

Organically modified silicates (ORMOSILS) or ceramics (ORMOCERS) [19], can be prepared when some organic groups are not hydrolysable during the network-forming polymerization process of metal alkoxides. Therefore, the reaction product is an organic-inorganic composite. These materials have mechanical properties intermediate between those of glasses and polymers. A schematic representation of the syntheses of the ormocers utilizing polydimethylsilane (PDMS) and TEOS was proposed by Wilkes is shown below [20]:

$$\begin{array}{c} OH \\ HO\text{--}Si\text{--}OH \\ OH \end{array} + \begin{array}{c} CH_3\ \ CH_3 \\ HO\text{-}(Si\text{-}O)_n\text{-}Si\text{-}OH \\ CH_3\ \ CH_3 \end{array} \text{------>} \begin{array}{c} OH\ \ CH_3\ \ CH_3 \\ HO\text{-}Si\text{-}O\text{-}(Si\text{-}O)_n\text{-}Si\text{-}OH \\ OH\ \ CH_3\ \ CH_3 \end{array} + H_2O \quad (2)$$

$$\text{Polymerization} \quad \text{----> } \begin{array}{c} O\ \ O\ \ CH_3\ CH_3\ \ O\ \ O\ \ O \\ \text{-O-Si-O-Si-O-(-Si-O-Si-O-)}_n\text{-Si-O-Si-O-Si-} \\ O\ \ O\ \ CH_3\ CH_3\ \ O\ \ O\ \ O \end{array} \quad (3)$$

Hydrolysis of TEOS first provides active monomers. The concentration of these monomers as a function of time define the distribution of different component in a condensation reaction. These reactions occur almost simultaneously and become more complicated when the organic component polycondenses with the inorganic component. It is of great importance to be able to determine the extent of the hydrolysis reaction in the TEOS component as well as the level of self condensation and network development of the final alkoxide species.

Several ormocer structures have been proposed by Schmidt and Wilkes [21,22]. The inorganic network can be modified by organic in two distinct ways. Organic can be crosslinked directly to the inorganic network via a chemical bond or the organic can be entrapped as molecules into the inorganic network.

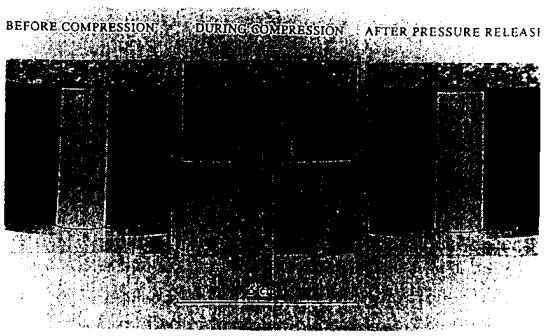

Figure. 3.12. Rubbery behavior of ORMOCERS

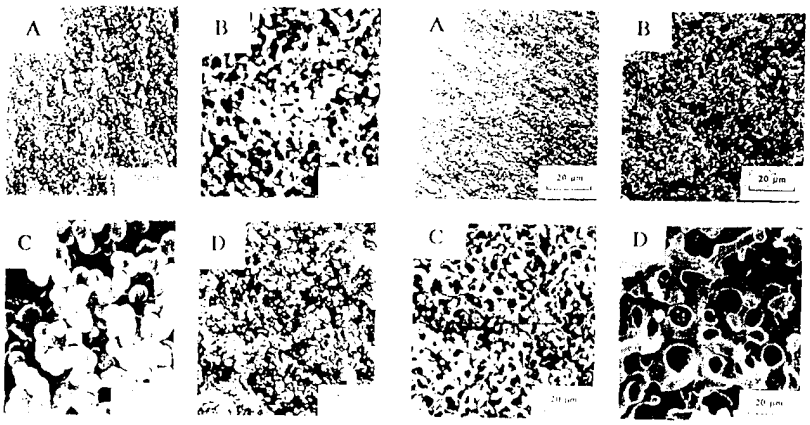

Figure 3.13 Microstructure of the ormocers can be tailored by many factors like reaction temperatures, water ratio, acid ratio, and organic/inorganic ratio.

One important structure-related property of the hybrid materials is the rubbery behavior as shown in Figure 3.12 [23]. The compression-release cycles were performed 500 times and there was no change in the state of the ormocers. Large monolithic ormocers with different shapes can be prepared without cracking. Due to the superior mechanical properties, films from submicron to few hundred micron have been prepared by ormocers solutions. Microstructure of the ormocers can be tailored by many factors like reaction temperatures, water ratio, acid ratio, and organic/inorganic ratio in very wide range (Figure 3.13) [24]. Porosity of ormocers can be changed from fully dense to more than 80% porosity. Therefore, ormocers are excellent low-temperature hosts for organic molecules and polymers. Organic components, either network formers or network modifiers, can be tailored for specific applications. Many organic polymer like laser dyes, non-linear optic polymers have been incorporated into ormocers for electronic and optical application. Contact lenses with good oxygen-permeability and hard coating on acrylic windows have also been fabricated by ormocers solutions. Other applications such as catalysis and sensors have been studied.

3.7. TiO_2 ORMOCER

The addition of TiO_2 into the ormocer has been frequently used to improve mechanical and optical properties, due to many superior properties of TiO_2, such as high refractive index, good thermal stability, and good nucleation agent. However, it is difficult to form a large monolith TiO_2 by the sol-gel process, due to the large shrinkage and poor mechanical properties of the dried gel. TiO_2 ormocer should be one of the best alternatives. Titanium oxide ormocer has also been

fabricated by reacting titanium alkoxide and polydimethylsiloxane(PDMS)[25].

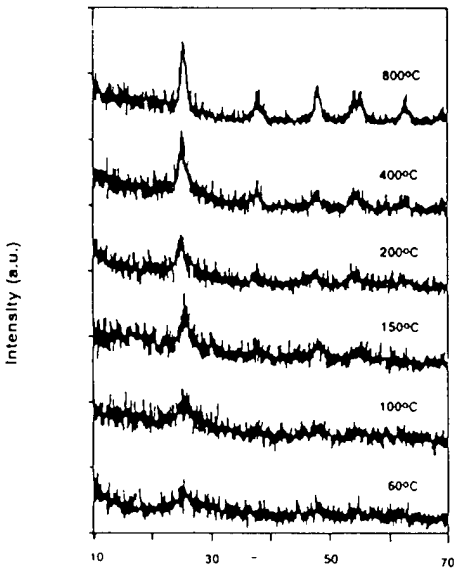

Figure 3.14 X-ray diffraction pattern of Ti ormocer after heat treatment at various temperatures.

Figure 3.14 shows the X-ray diffraction patterns of the sample with Ti/PDMS= 23/1 after heat treatment at different temperatures. The crystalline phase became apparent after curing at 150°C. The crystalline phase of the samples is identified to be hexagonal anatase-TiO_2. At low temperatures, the crystallite particle size of the material are too small to be detected using X-ray diffraction. For binary TiO_2-silicates ceramic, the anatase phase does not become apparent until very high temperatures (>700°C). However, by preparing organically modified titania oxide , the anatase TiO_2 phase is stable through the temperature range of 150°C to 800°C. The porosity of this TiO_2 ormocer has not been studied, however, it should be very high due to the microstructure nature of the ormocer materials.

3.8 Aerogel through Supercritical Drying

Considerable shrinkage and reduction in surface area and pore volume is usually observed during drying by evaporation. This may be a result of continuing condensation reactions between terminal -OH groups and/or surface tension induced collapse. The capillary pressure generated during drying is related to the pore fluid surface tension, γ_{lv}, and contact angle, θ, between the fluid meniscus and pore wall as follows,

$$Pc=-(2\gamma_{lv}\cos\theta)/a$$

where a is the pore radius. The supercritical pore fluid extraction method of aerogel synthesis involves elimination of capillary pressure to avoid the deformation of wet gel during drying.

To remove the liquid in the gel, several extraction methods can be employed. Normal drying leads to capillary tensions as the vapor/liquid interface retreats into the porous structure. The resulting shrinkage (and cracking) of the gel network proceeds until the densified structure is able to withstand these forces. Shrinkage can be reduced by prolonged aging, by aging with additional catalyst, or by using chemical additives (DCCAs). This can be also achieved, if the liquid-vapor phase transition is avoided by removing the solvent supercritically. The typical path followed during supercritical drying (SCD), is shown in the phase diagram of Figure 3.15.

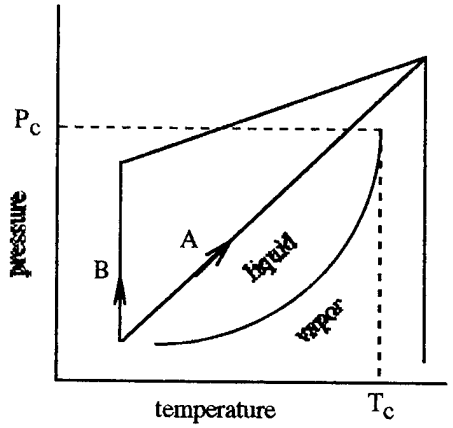

Figure 3.15. Temperature-pressure paths during supercritical drying. The conventional path (A) makes use of a totally filled autoclave; (B) corresponds to the case of nitrogen prepressure. Above the critical point of the solvent (Tc,pc) capillary tension ceases.

Hereby the gel is put in a pressure vessel (an autoclave). Then the pressure and the temperature are raised above the critical point of the solvent. As in a supercritical fluid, liquid and vapor phase become indistinguishable, no capillary forces occur. After releasing the fluid through the outlet valve and subsequent cooling, the aerogel can be taken from the autoclave. It is important that enough solvent is provided in order to guarantee supercritical conditions throughout the whole drying process; otherwise shrinking and cracking will occur. Often the autoclave is pre-pressurized with nitrogen to prevent premature evaporation of the solvent.

Supercritical drying can be performed safely near ambient temperatures, if the pore liquid is exchanged for a liquid with a lower critical temperature, as e.g. carbon dioxide (T_c=31.0°C, P_c=73.9 bar). Depending on sample size, a complete solvent exchange may require a long time. A pre-exchange with an intermediate solvent can be helpful; this is particularly important, if components of the solvent and the liquid used for SCD are not miscible, as for instance water and CO_2.

3.9 Aerosol Synthesis of Fine Powders

Aerosol reactors offer an attractive alternative to conventional powder synthesis methods. High purity powders can be obtained using molecular precursors as starting materials. Narrow, uniform powder size distributions can be achieved by controlling particle nucleation and growth rates. A schematic of the aerosol reactor is shown in Figure 3.16. Powders with surface area as

high as 500 m^2/g can be achieved by controlling hydrolysis of the sol-gel solutions and processing conditions. Aerosol process can provide high quality fine powders with a low-cost and continuous process comparing to the conventional methods.

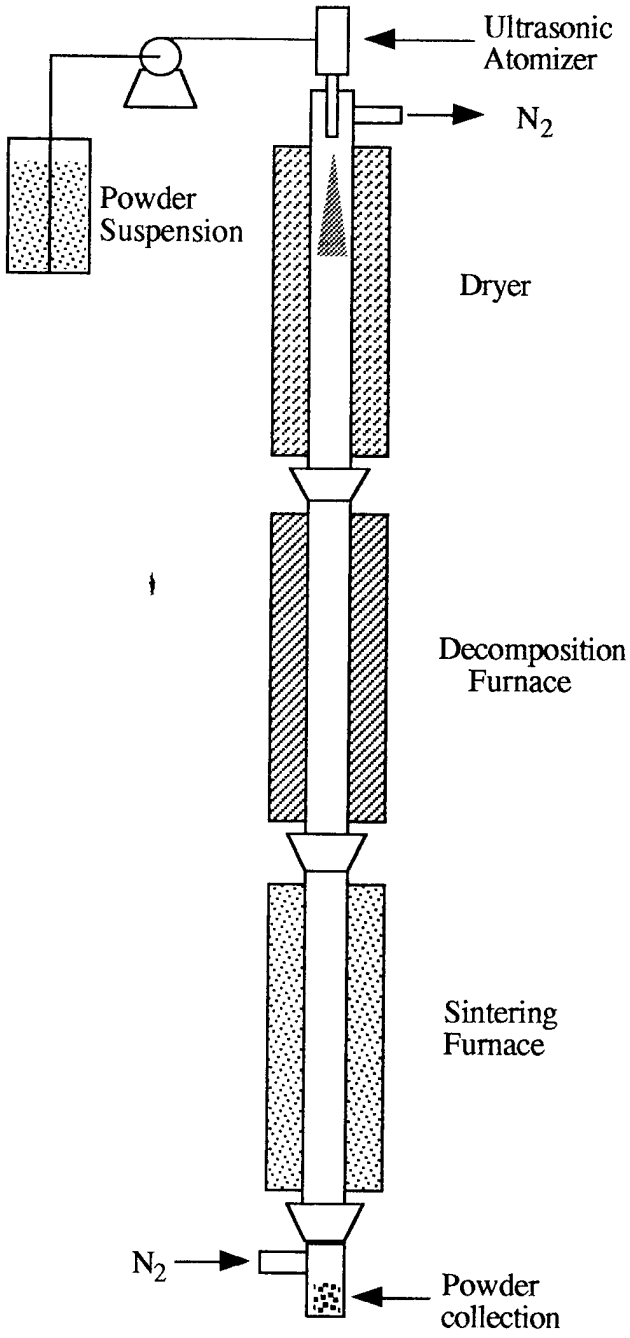

Figure 3.16. A schematic description of aerosol reactor.

3.10. Summary

As discussed above, the efficiency of photochemical reactor for degradation of toxic and

hazardous chemical substances is dependent on several factors: 1) Specific surface area, particle size and pore size of TiO_2 material, 2) Surface state and morphologies of TiO_2 material, 3) The crystallographic phase of TiO_2 , 4) Doping effect, 5) Light harvestivity or dye-sensitization, 6) Translucency of photocatalyst, and 7) Kinetics of photoredox processes.

The anchoring of charge transfer dyes to wide band gap TiO_2 semiconductor renders it sensitive to visible light. In addition, the rate constants for electron injection from Ru complex to TiO_2 is much higher than that of recombination. The addition of WO_3 or MoO_3 increase the catalysts surface acidity, therefore increasing remarkably the photocatalytic activity. In very fine particles, the diffusion of charge carries from the interior to the particle surface can occur more rapidly than their recombination. When the particle size decreases down to a 50 Å, quantum size effect should be taken into account. It is feasible to obtain quantum yields for photoredox processes approaching unity. Titania-silica (TiO_2-SiO_2) aerogels or TiO_2 ormocer have been proven to have high translucency, therefore it will have higher efficiency in the photocatalytic oxidation.

IV. EXPERIMENTAL

4.1. TiO_2 Material Processing

In Phase I program, TiO_2 photocatalyst in the forms of powders, granules, and films, has been prepared by various methods, such as conventional sol-gel route, aerosol, and aerogel process.

A. Sol and Gel Preparation

Method 1: Direct Hydrolysis of Titanium Alkoxides

One mole of $Ti(^iPrO)_4$ in 5 mole of isopropanal follows by adding various moles of water that diluted in i-propanol under the stirring. The resulting white milky solutions are titanium hydroxide colloid solutions.

Method 2: TiO2 sol solutions for monolithic gel

TiO_2 sols were prepared by taking the molar ratio between the reactants as: 1 $Ti(O^iPr)_4$: 20 ethanol : 4 H_2O : 0.08 HNO_3. Titanium isopropoxide was mixed with the anhydrous ethanol at room temperature, and added to a solution of ethanol + deionized water + 70% nitric acid. The transparent monolithic gel was obtained in less then 5 minutes. The same process is followed to make WO_3 doped TiO_2 transparent monolithic gel, by mixing tungsten isopropoxide with titanium isopropoxide and ethanol at the beginning.

Method 3: Polymeric titanium alkoxides

Polymeric titanium alkoxide was prepared by adding one mole of acetic acid (or 2-ethylhexanoic acid(2-EHA)) to 1 mole of $Ti(ButO)_4$. An exothermic reaction takes place, leading to a clear solution. Four moles of water, diluted in isopropanol, are then added under the stirring. The viscosity of the solution increases slightly, shows certain polycondensation was happened. After distilling the solvents, viscous ploymeric titanium alkoxides can be achieved.

Acetic acid reacts with metal alkoxides, increasing the coordination and decreasing the chemical reactivity of metal alkoxides.

$$Ti(OBu^n)_4 + AcOH \text{ ---> } Ti(OBu^n)_3OAc + Bu^nOH$$

Acetate groups behave as bidentate ligands, giving rise to chelating and bridging species. The chemical reactivity of the precursor decreases, avoiding TiO_2 precipitation when water is added. Water first removes the (OBu^n) ligands while chelating acetate remains bonded to the titanium, slowing down both hydrolysis and condensation processes.

B. TiO_2 Material Fabrication

Method 1: Conventional sol-gel route and heating gun treatment

Sol solutions or gels were first dried with heating gun and then sintered using conventional furnace in air to get TiO_2 powders. The heating gun provided large air flow to dry the gels more efficiently.

Method 2: Aerosol route

The simplified aerosol reactor for the preparation of TiO_2 powders in the Phase I study is shown in Figure 4.1. Various solution precursors has been tried including precipitation sol, colloid solution and ground gel powder aqueous and alcoholic sol. The BET surface area of powders varied from 120 to 250 m^2/g for the preliminary study. Further research should be able to improve the productivity and surface area. The new design of aerosol reactor is progress.

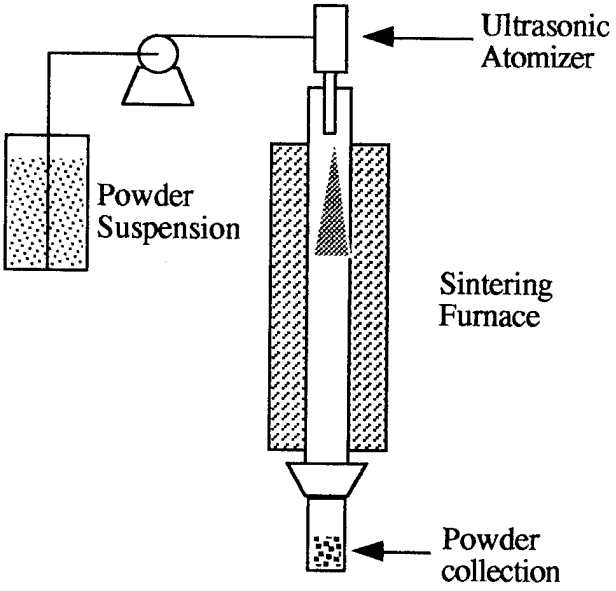

Figure 4.1. Aerosol reactor.

Method 3: Aerogel technology

In order to prevent densification of the gels and maintain high porosity, supercritical drying methods were used to dry the solvent filled gels to become aerogels.

TiO_2 sols were prepared by taking the molar ratio between the reactants as: 1 $Ti(O^iPr)_4$: 20 ethanol : 3 H_2O : 0.08 HNO_3. Titanium isopropoxide was mixed with the anhydrous ethanol, at room temperature and and added to a solution of ethanol + deionized water + 70% nitric acid. The transparent monolithic gel was obtained in less then 5 minutes. Different mole ratio of tungsten isopropoxide was mixed with titanium isopropoxide and ethanol at the beginning to study the

doping effect.

The monolithic gels were exchanged the original solvent with acetone after certain aging time. An alternate low temperature extraction of carbon dioxide was performed after exchange of the original solvent. The monolithic gel was placed in the container. The autoclave is filled with additional acetone and sealed. The liquid carbon dioxide was used to exchange the acetone with the pressure increases of about 120 bars and excess pressure above that is released. After totally exchange of acetone by liquid carbon dioxide, the pressure is released from the vessel. The autoclave is then purged with air. The supercritically dried gel is translucent.

Method 4. Aero-ormocer

Polymeric titanium alkoxide was prepared by adding one mole of acetic acid (or 2-ethylhexanoic acid) to 1 mole of $Ti(ButO)_4$ as that has been mentioned in the method 3 of sol and gel preparation. A small amount of polymeric titanium alkoxide (10 to 30 mol%) can be mixed with TiO_2 sol solution, a monolithic transparent TiO_2 ormocer is obtained within several minutes. A TiO_2-SiO_2 ormocer has also been prepared by adding small amount of polydimethylsiloxane (PDMS, 10-30 mol%) to titanium isopropoxide sol followed by the same processing condition described previously for TiO_2 ormocer, a monolithic transparent TiO_2-SiO_2 ormocer is also obtained within several minutes.

Supercritical drying by carbon dioxide can be performed on these TiO_2 ormocers, aero-ormocers can be achieved. The TiO_2 Aero-ormocer is actually the same material-porous TiO2 with anatase phase as the TiO_2 aerogel if annealing at high temperature after all the organic part decomposited. Compare to aerogels, aero-ormocers provide better mechanical properties than aerogels. After supercritical drying and annealing at high temperature, aero-ormocers, especially TiO_2-SiO_2 aero-ormocer, can maintain the shape without cracking, thus monolith or granular of aero-ormocers can be made easily. The BET surface area of aero-ormocers showed about the same as that of aerogel, providing the similar microstructure as the aerogel.

In summary, sol-gel derived TiO_2 materials can be fabricated through four processing methods : i) conventional sol-gel route, ii) aerosol, iii) aerogel, and iv) aero-ormocer. The first two techniques are low-cost compared to aerogel technique. However, the aerogel and aero-ormocer process provide materials with better properties and performance.

C. TiO_2 Film

The TiO_2 films were deposited on transparent Microscope Cover Glasses (Fisher) by dip-coating in organic acid modified TiO_2 sol followed by heating gun drying and sintered in furnace at 550°C for 15 minutes. Crack-free coatings up to about 1 μm have been achieved.

TiO_2 ormocer coatings have been prepared on the ITO glass substrates, after supercritical

drying, aero-ormocer thick films up to few ten μm have been achieved. The surface morphology of this aero-ormocer coating showed identical as that of the aerogel from scanning electron microscopy. More systematic study need to be done on this aero-ormocer thick films.

D. Dye-sensitizing TiO_2 Powder

The dye sensitization of TiO_2 powders were prepared by immersing the TiO_2 materials(powders, granules, monoliths, or coatings) in Ru dye solution (10 mg of $[RuL_2(m\text{-}(CN)Ru(CN)L'_2)_2]$ in 100 ml EtOH) and either let it soak up solution for more than 12 hours, or heat up solution to reflux for 2 hours. After drying, the dye-sensitized TiO_2 materials turned dark wine red in color. Only about 10mg of this Ru dye is needed to sensitize 100 g of TiO_2. The Ru-dye was purchased from Solaronix SA., Switzerland in a pure powder form. Small amount of this Ru dye was also synthetized in house to confirm the result.

E. Tungsten doping

Tungsten doping was induced into TiO_2 by sol-gel route at sol preparation step. Tungsten (VI) isopropoxide, $W(O^iPr)_6$, mixed with titanium isopropoxide followed by mixing with the anhydrous ethanol, at room temperature and and added to a solution of ethanol + deionized water + 70% nitric acid. The transparent monolithic gel was obtained in less then 5 minutes. The wet gel then was heat treated using heating gun to get white powder or put into autoclave to get dried bulk porous gel. One of the advantages of sol-gel process is the adjustable chemical composition and molecular level mixing. The tungsten doping is expected to be more homogeneous through out this sol-gel derived TiO_2 matrix, comparing to the traditional route of immersing TiO_2 matrix into tungsten compound and then heat treated in air. That should resulted in higher doping efficiency for this sol-gel derived TiO_2.

4.2. Analysis of microstructure and crystallography

The development of crystallographic phase as a function of the thermal treatment temperature was determined by x-ray diffraction (XRD). The microstructures of TiO_2 powder, film and aerogel were investigated using transmission electron microscopy (TEM), and scanning electron microscopy (SEM). Analysis of specific surface area of TiO_2 materials was carried out by Brunauer-Emneth-Teller method (BET).

4.3. Characterization of photodegradation of chemical wastes

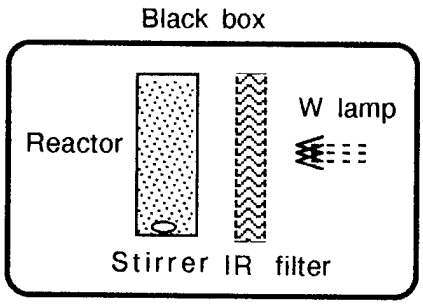

Figure 4.2. The photocatalytic reactor with tungsten lamp as light source and water as IR filter.

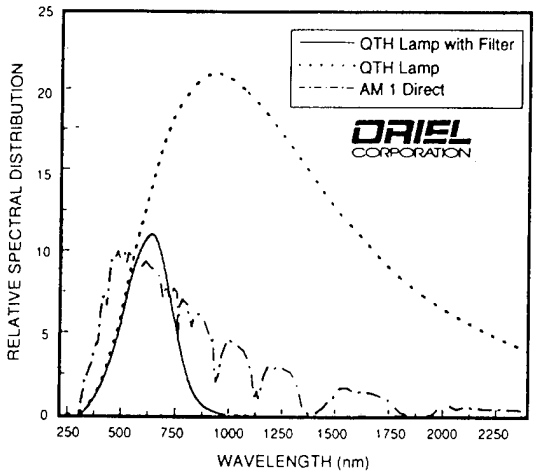

Figure 4.3. Spectrum of 3300K tungsten halogen lamp. Filtering removes a lot of the excess IR, but is inefficient and leaves a UV deficit. (OAIEL corp.)

The TiO_2 powders or granulars are suspended by magnetic stirring in a custom-made photocatalytic reactor, as shown in Figure 4.2. The light source is a 300W tungsten halogen lamp (GRAINGER) with water IR filter. Figure 4.3 shows typical solar spectrum and tungsten lamp spectrum. Filters can be used to modify the spectrum to make a reasonable, but inefficient match in the visible and leaves a UV deficit. The characterization of conversion of chemical waste is carried out at Aton Laboratory, Inc. using gas chromatography (GC) methods. No decreasing of 4-CP concentration was tested from a blank-run of 4-CP solution under the exposure for 1 hour.

V. RESULTS AND DISCUSSION

In this section, the achievement of high photocatalystic efficiency of degradation of 4-chlorophenol and dimethyl methyl phosphonate (DMMP) in Phase I research is summarized. The innovative technologies developed in Phase I work and their resulting on properties of TiO_2 materials are described and discussed. Their implications on efficiency of photodegradation of chemical waste are presented.

5.1 Specific surface area

A. Conventional sol-gel route and heating gun treatment

The final specific surface area is dependent on annealing temperature, as shown in Figure 5.1. The annealing temperature lower than 350°C dose not affect the specific surface area of the powder. The surface area is decreased to half at the temperature above 400°C.

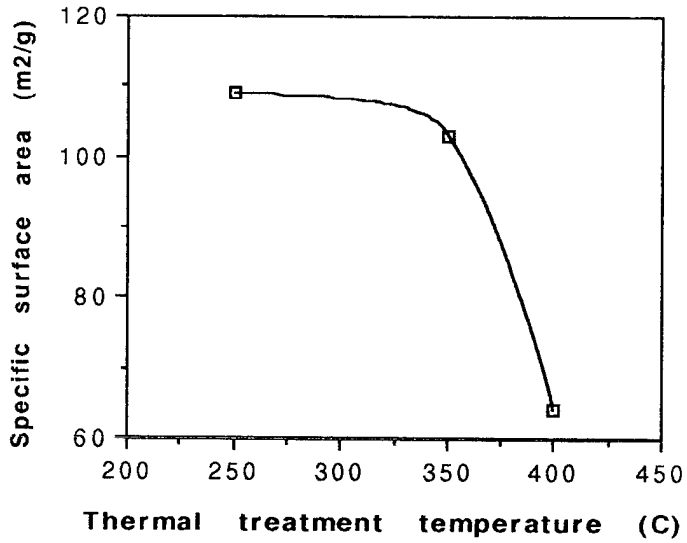

Figure 5.1. Specific surface area as a function of annealing temperature with 4 mole of water per mole of titanium.

The specific surface area of the powder is found also depending on the water content during sol preparation. Figure 5.2 shows the specific surface area of TiO_2 powder with different water content during sol preparation. The samples were annealed at 400°C for 10 minutes in furnace. The specific surface area of the TiO_2 powder increased with increasing water content in these conditions. Up to 240 m^2/g of specific surface area of TiO_2 powder can be achieved by carefully controlling the sol preparation condition.

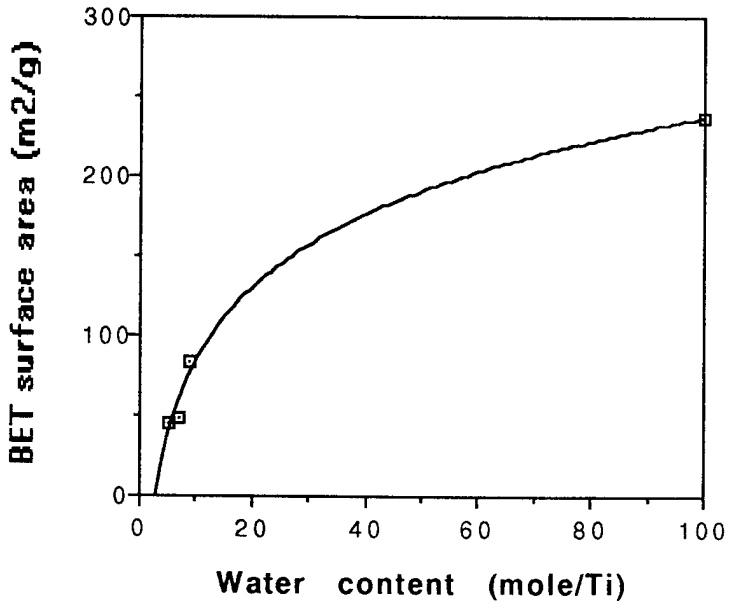

Figure. 5.2. The surface area of TiO_2 powder as a function of water through conventional sol-gel route. The samples were annealed at 400 °C.

B. Aerosol Route

The results from preliminary investigation is permissible. The white powder has been

obtained using ground gel aqueous sol spouting into furnace with temperature of 500 °C. The specific surface area is 240 m^2/g. The conversion of 4-CP increased 80% compared with Degussa P25 TiO_2 powder under the same treatment condition (see section 5.4).

Other solvents such as MeOH and ^iPrOH has also been tried at different furnace temperatures. The black powder was obtained and the conversion of 4-CP is almost zero. The further study on processing conditions should be done by varying the solvents, concentration of the sol and furnace temperature.

C. Aerogel Technique

The BET surface area and weight loss as a function of the annealing temperature of aerogel granules are shown in Figure 5.3. The simple calculation based on weight loss data indicate that the gel has almost hydrolyzed to become titanium hydroxide. The surface area decreased with increasing annealing temperature, but it still very large.

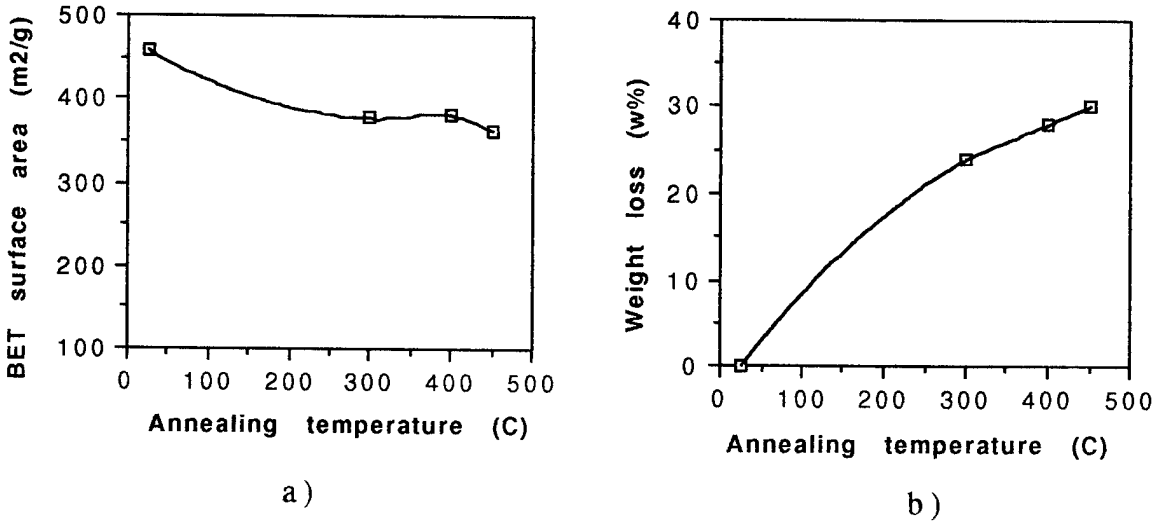

Figure 5.3. a) BET surface area and b) weight loss of aerogel powder as a function of annealing temperature.

Table I lists the range of BET surface area of the TiO_2 powder prepared using various methods. The very large surface area of TiO_2 powder up to 460 m^2/g can be obtained by using aerogel method. In conventional sol-gel process, large surface area of TiO_2 powder can also be obtained by increasing water content. Aerosol method is a low cost process and can reach relatively large surface area, as show in table I. The BET surface area of TiO_2 powder achieved in this study is 3 to 9 times larger than that of commercial TiO_2 powder (Degussa P-25 powder, surface area = $50m^2/g$).

Table I. BET surface area of TiO_2 powder via various methods

	Preparing route			
	conventional sol gel	aerosol	aerogel	aeroormocer
BET surface area (m^2/g)	40 - 240	120 - 250	360-460	310 - 430

5.2. Crystallographic Phase development as a Function of Temperature

The crystallographic phase development as a function of annealing temperature of TiO_2 powder is shown in Figure 5.4. Anatase phase forms at temperature lower than 360°C, and only trace amounts of rutile phase can be observed by XRD analysis. Pure rutile can be obtained at temperature higher than 650 °C. Anatase/rutile crystallographic phases coexist in the middle temperature range. The highest conversion efficiency of 4-chlorophenol is obtained by using the powder sintered in this temperature range (450 to 550°C), as discussed later.

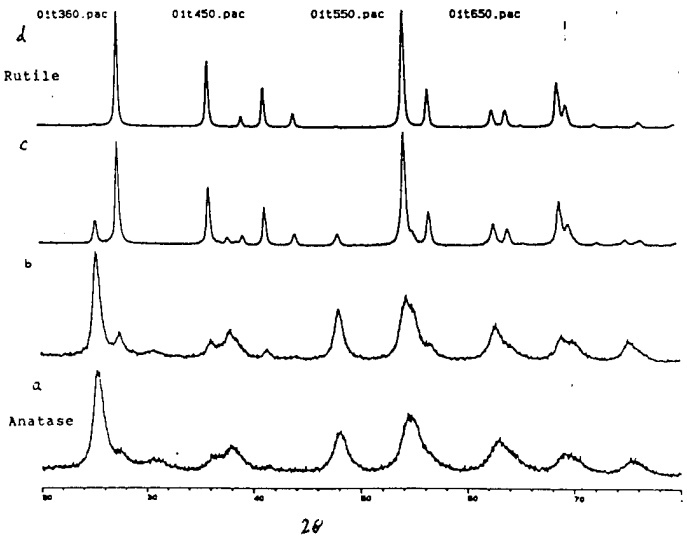

Figure 5.4. Crystallographic phase development as a function of the temperature. TiO2 powder were annealed at a) 360°C, b) 450°C, c) 550°C and d) 650°C.

5.3. Microstructure of the TiO_2 materials

The particle size and surface morphologies of various TiO_2 materials are quite different. Figure 5.5 shows two examples (SEM image). Aerosol powder is an aggregation of fine particles.

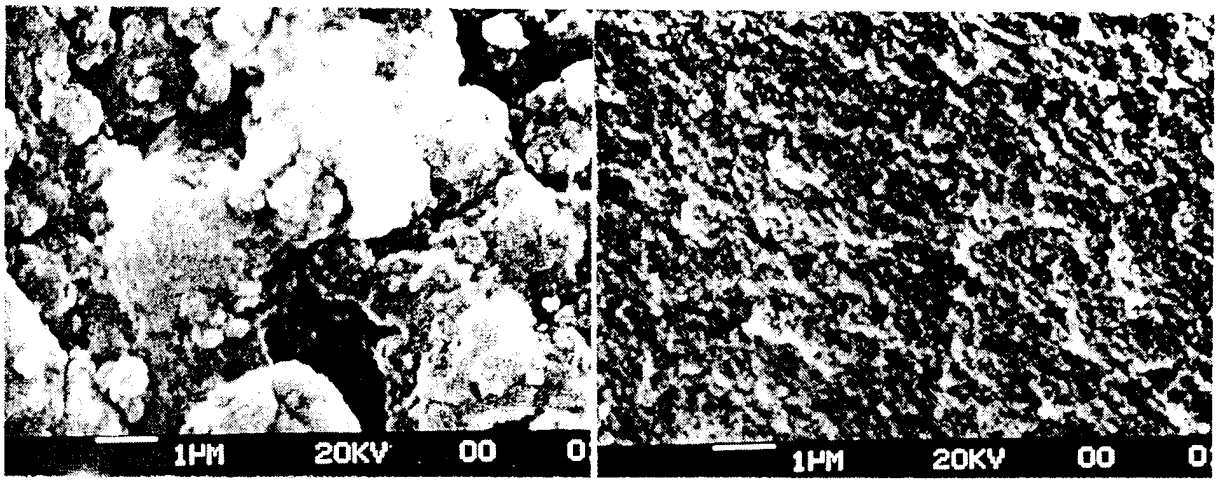

a) Aerosol powder b) Aerogel powder

Figure 5.5. Surface morphologies of TiO_2 powders made from:
a) aerosol, and b) aerogel methods.

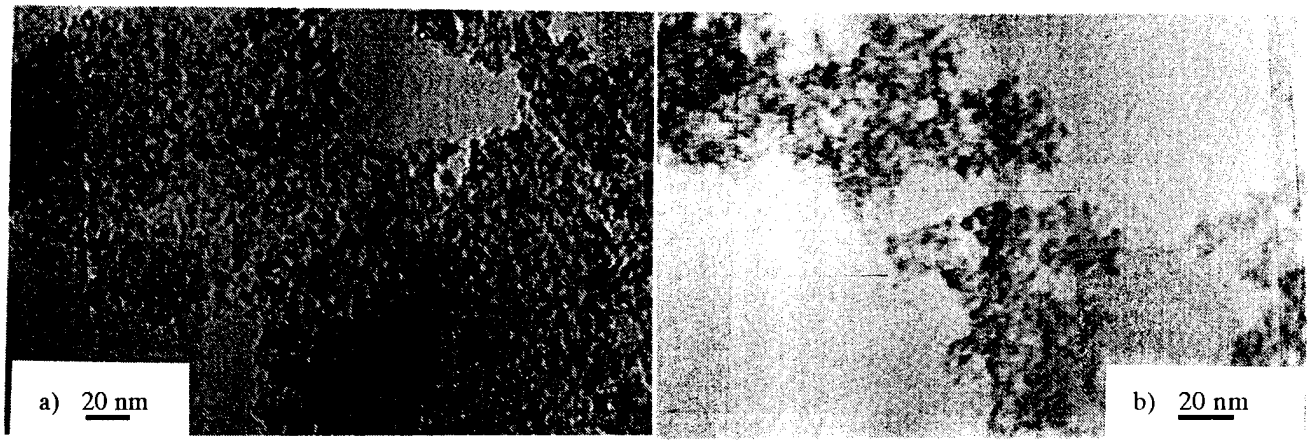

Figure 5.6. TEM micrographs of TiO_2 particles made from:
a) aerosol, and b) aerogel methods

Aerogel is also an aggregation of fine particles with very porous structure. Figure 5.6 shows TEM micrographs of these two samples. The particle size of aerosol is about 60 Å, while the aerogel is

about 25Å, all with very uniform particle size. The effect of surface morphology of TiO_2 powder on the conversion efficiency of chlorinated hydrocarbons should be studied in the future.

5.4. Photodegradation of 4-chlorophenol aqueous solution

A. Photocatalytic activity of various TiO_2 powders

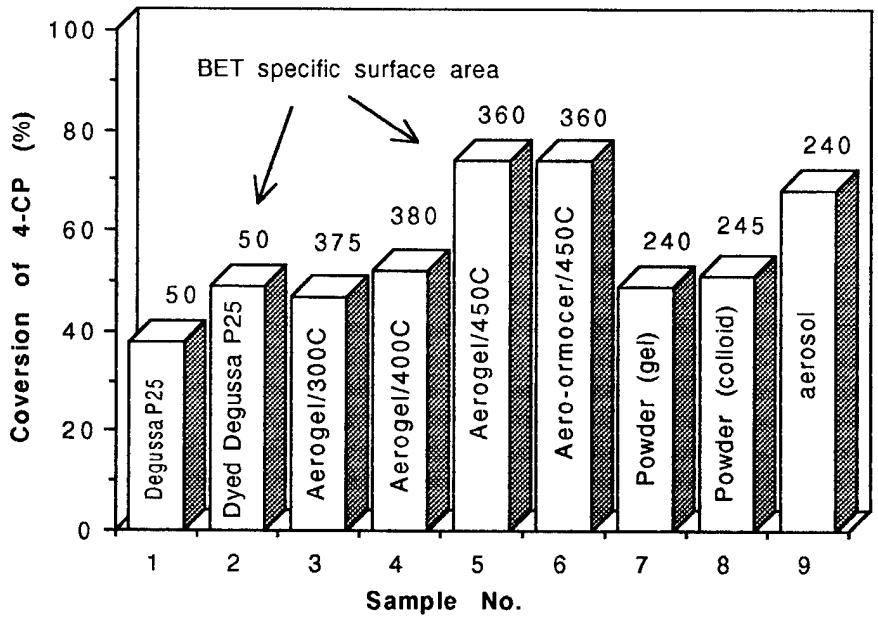

Figure 5.7. Comparison of efficiency of converted 4-CP of various samples.

Figure 5.7 shows comparison of the conversion percentage after reacting for 20 minutes for some of the typical samples that have been prepared in this study. As a comparison, Commercial TiO_2 powder (Degussa P25) is used as a standard. The dye sensitized Commercial TiO_2 is prepared by immersing the powder in Ru dye solution for 12 hours as that has been described previously. As shown in Figure 5.7, photocatalytic conversion of waste chemical increased about 30% by using dyed powder after reacting for 20 minutes. The larger surface area powders made in this study show higher conversion rate. However, the BET surface area is not only effect on the efficiency of photodegradation, as mentioned at beginning. Even though, the BET surface area of aerogel decreases as increasing annealing temperature, the conversion rate increased; thus should be related to the increasing anatase phase for aerogel with higher annealing temperature.

B. Effects of Tungsten Doping

Figure 5.8 shows photocatalytic conversion of 4-CP as a function of tungsten doping

concentration for TiO_2 powder by the conventional sol-gel route. The concentration of WO_3 which gives maximum photocatalytic activity was about 3 mol%, and more than 65% increase in conversion percentage has been achieved.

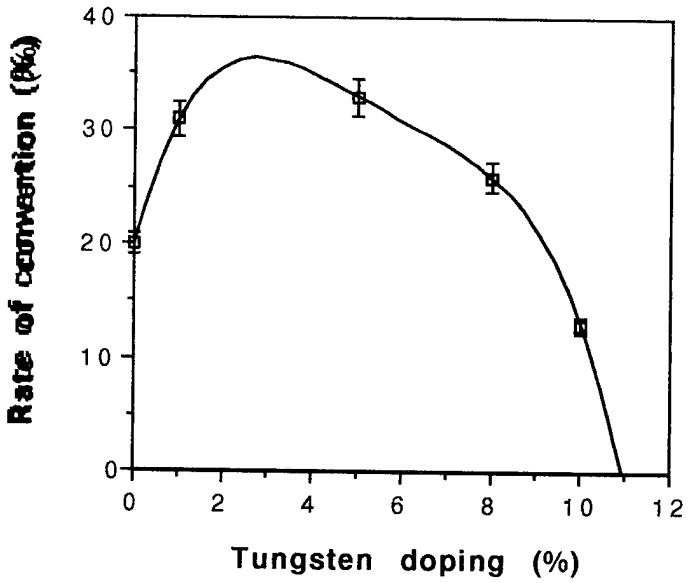

Figure 5.8. 4-CP conversion rate using TiO_2 powder as a function of tungsten doping concentration.

C. Dye-sensitized TiO_2

The dye sensitization of TiO_2 materials was carried out by immersing the powders or granulars in Ru dye solution (10 mg in 100 ml alcohol for 100 g TiO_2) for 12 hours. We found that photocatalytic conversion percentage of 4-CP increased about 35% after 20 minutes reaction by using dyed Degussa P25 TiO_2 powder. For high surface area TiO_2 aerosol powders with 10% tungsten doping, the photocatalytic conversion percentage of 4-CP increased from 13% to 40% by using dye-sensitized power under same illumination conditions; which means more than 3 times increase of conversion percentage can be achieved.

D. Photodegradation as a function of time

The conversion rate of chemical waste is an important data for design of reactors. Figure 5.9 shows the conversion of 4-CP as a function of exposure time. For comparison, commercial TiO_2 powder Degussa P25 was also measured in the same condition. 0.4 gram of powder is suspended in 60 ml 4-CP solution by magnetic stirring in a custom-made photocatalytic reactor. Other conditions are same as described at the beginning of this section .

The sample N.1 is prepared using conventional sol-gel route followed by heating gun treatment with 5 mol% of tungsten doping. As shown in Figure. 5.9, 48% of 4-CP was converted

using Chemat TiO_2 powder after reacting for 20 minutes. In general, conversion rate of chemical waste follows the empirical form[26]:

$$[4\text{-CP}\%]=\exp[-\alpha t]$$

where [4-CP%] is non-reacted percentage of 4-CP, t is exposure time and α being a constant which equals the product of conversion efficiency, absorbed light intensity and oxygen adsorbed. Since the reaction rate is much higher at the beginning of the reaction, therefore a three-step of unit is proposed in Phase II program which will discussed in Phase II work Plan.

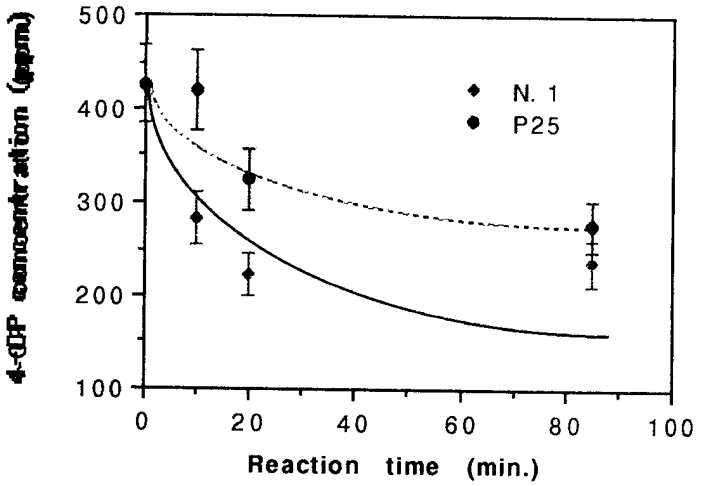

Figure 5.9 The conversion of 4-CP as a function of exposure time in comparison with Degussa P25.

E. TiO_2 aerogel and aero-ormocer

Porous TiO_2 materials (powders, granule and monoliths) from either aerogel and aero-ormocer process showed extremely high surface area. Surface area as high as 360 m2/g can be achieved even after sintering at high temperature. The photocatalytic activity also shows significant improvement comparing to TiO_2 powders by other processing techniques. After reacting for 20 minutes, conversion percentage of 4-CP can be as high as 77% comparing to the 37% by the commercial powder. Dye-sensitized effect on aerogel has also be studied. The conversion percentage after 10 minutes can be improved from 46% to 62%, but after 20 minutes are the same at 77%. This may be due to the already high conversion percentage of the aerogel materials that improvement by dye-sensitized effect is not easy to identify. TiO_2 from either aerogel or aero-ormocer shows about the same photocatalytic activity, due to the identical chemical composition and microstructure after high temperature annealing. However, larger size of granule or even monolith can be easier to achieved from the aero-ormocer process by controlling drying and annealing process. The TiO_2-SiO_2 aero-ormocer also showed similar photocatalytic activity as that of aerogel, even though small amount of SiO_2 has been introduced into the TiO_2 matrix. This TiO_2-SiO_2 aero-ormocer also showed better mechanical strength, while larger size of granule or even monolith can be easier to achieved.

F. TiO_2 film

The photocatalytic activity of TiO_2 films that deposited on transparent Microscope Cover Glasses with 1"x1" area and sintered in furnace has been studied. The conversion percentage of 4-CP of the films was in the range of 23 to 33 % depending on the sintering temperature. Although the conversion percentages are relatively low, but comparing to the amount of TiO_2 on the films, the efficiency is actually impressive. TiO_2 aero-ormocer coatings have been prepared on the ITO glass substrates with 1"x1" size and about 10μm thick. About 39% of conversion percentage can be achieved, which can be significantly improved if more systematic study has been made.

5.5. Photodegradation of DMMP

Army is particularly interested in destroying explosives and the chemical agent simulants such as dimethyl methyl phosphonate (DMMP). The photoelimination of DMMP in MeOH was tested using Degussa P25 and high specific surface area sol-gel TiO_2 (300 m^2/g) with 5 mol% of tungsten doping fabricated in this study(N. 1). The powder is suspended in 2310 ppm DMMP methanol solution by magnetic stirring in a custom-made photocatalytic reactor and exposured for 20 minutes. The efficiency using tungsten doped high surface area powder is much high than that using Degussa P25 TiO_2 powder, as shown in Table II.

Table II. Photoelimination of DMMP analysis by GC

	original	Degussa P25	N. 1
concentration (ppm)	2310	2280	<1000

The DMMP concentration after reacting with N.1 powder is below detection limit of the GC column (<1000ppm). The efficiency for elimination of DMMP using TiO_2 powder with high specific surface area and tungsten doping is much higher compared to that of commercial powder (more than 40 times higher). The improvement of efficiency between N1 and commercial powder for elimination of DMMP is much high than that for elimination of 4-CP in aqueous solution(about 2-3 times). This may be due to that DMMP has more complex structure compared to 4-CP, and requires more efficient photocatalyst to decompose. As in the case of elimination of salicylic acid[27], 10 times improvement of efficiency has been reported by using high surface area TiO_2 powder.

Another possible reason for this is due to different surface area and using MeOH as a solvent. As discussed in section 3.1, oxidative electron transfer occurs exclusively through a surface-bound hydroxyl radical, $\{>TiOH^{\bullet}\}^{+}$ or equivalent trapped hole species. Degussa P25

powder is stoichiometric TiO_2. The TiOH radical might exist in the titanium oxide powder through sol-gel route thermal treated at low temperature. This may enhance the oxidation of chemical waste, especially in the case of non-aqueous solution.

5.6 Discussion and Summary

A technology of the elimination of toxic and hazardous halogenated hydrocarbons with potential low-cost and high volume process has been developed in this Phase I study by using TiO_2-photocatalyst under the simulated solar irradiation with UV deficit.

TiO_2 materials by the sol-gel process with large BET surface area up to 460 m_2/g has been obtained by aerogel process. The efficiency of photocatalytic decomposition of 4-chlorophenol (4-CP) aqueous solution has been improved significantly comparing to that of Degussa P25 (with specific surface area of 50±15 m^2/g). The photocatalytic conversion of TiO_2 powder made from aerosol, aerogel, and aero-ormocer is almost double of that of Degussa P25 at same irradiation and exposure time. The specific surface area of our samples can be ten times larger than that of Degussa P25. The efficiency increases about 3 times. It is also true by comparison of our own samples. For example, The BET surface area of aerogel ($360m^2/g$) is 44% larger than that of aerosol (250 m^2/g), the conversion percentage of chemical waste only increase 8%. One of the reason is the conversion percentages are too high to compare (77% to 69%). The other reason may be, as mentioned before, due to that the efficiency not only depend on the surface area, but also depends on interfacial electron-transfer rate constant and electron-hole recombination rate. The surface defect and morphology also place very important role in photocatalytic reactivity.

As we have mention previously, by coating a small amount of sensitized dye (about 1 mg dye per 20 g TiO_2) the conversion of chemical waste in visible light improved by 35% using commercial Degussa P25 TiO_2 powder. However, the conversion percentage of chemical waste can increase from 13% to 40% using dye-sensitized high surface area TiO_2 powder with 10 mol% of tungsten doping under same illumination conditions. The conversion of chemical waste increased more than 3 times at same irradiation and exposure time.

Tungsten doping has also been proven to be effective on increasing the conversion efficiency. The conversion of chemical waste was improved by more than 60% using 5 mol% of tungsten doped TiO_2 powder.

These effects can be much higher in the case of more complex compounds such as DMMP and salicylic acid. Another possible reason for this is due to different surface area and using MeOH as a solvent. As discussed in section 3.1, oxidative electron transfer occurs exclusively through a surface-bound hydroxyl radical, $\{>TiOH^{\bullet}\}^{+}$ or equivalent trapped hole species. Degussa P25 powder is stoichiometric TiO_2. The TiOH radical might exist in the titanium oxide

powder through sol-gel route thermal treated at low temperature. This may enhance the oxidation of chemical waste, especially in the case of non-aqueous solution.

From comparison with SiO_2 aerogels, for which surface areas of up to 1000 m^2/g were reported. We believe that, by optimizing the preparation conditions, a larger surface area can be achieved for the TiO_2 aerogels and aero-ormocers. Aerogel process for small quantity is relatively high cost. But the cost estimation for larger quantity or industrial production of aerogel has identified the major factor of the overall cost is the starting materials (Figure 5.10)[28]. The operation cost is relatively low even comparing to other industrial process for powders and ceramics. Actually, SiO_2 aerogel has been mass production with low cost for years. Titanium alkoxides are relative low cost raw materials, therefore, Ti aerosol, aerogel and aero-ormocer can be expected as low cost materials after scaling up.

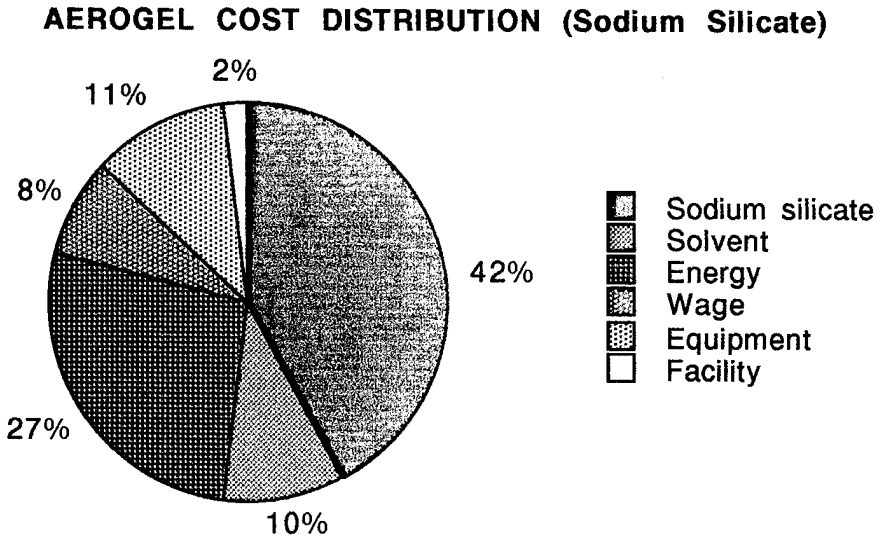

Figure 5.10 Relative silica aerogel production costs using sodium silicate as precursor.

In summary, the improvement of photocatalytic efficiency has been achieved by: 1) increasing the surface area of the powder, 2) using dye to sensitize the powder to visible light, 3) adding doping to change the density of surface hydroxyl group, 4) amorphous phase might increase the radiation harvestivity and 5) the oxidation of chemical waste might be enhanced by existing the surface state such as TiOH.

VI. CONCLUSIONS

The goal of Phase I project is to demonstrate efficient solar photocatalytic degradation of chemical waste such as 4-CP. In Phase I project, we used tungsten halogen lamp as an irradiation source under IR filter, which leaves a UV deficit. Therefore, the efficiency measured in Phase I research can be expected being lower than that obtained under solar irradiation.

In Phase I work, we demonstrated that photocatalytic efficiency can be increased by: 1) increasing specific surface area of TiO_2 material, 2) dye-sensitizing TiO_2 material, 3) transition metal doping and, 4) suitable crystallographic phase and morphologies. Estimation of effects of various parameters on activity from the results in Phase I work lists in Table III. Even though ten times larger surface area of TiO_2 powder has been obtained comparing with Degussa P25 powder, the increase of reactive rate observed in Phase I research is about 3 times. Reactive rate of dye-sensitized TiO_2 powder can increase from 1.4 (Degussa P25) to 3.5 times (high surface area powder with 10 mol% of tungsten doping). Adjustment of anatase/rutile phase can improve the reactive rate by 2 times. The improvement of reactive rate by tungsten doping can be 1.6 times. Even morphology of the powder can affect by factor of 1.5. From this roughly estimation, it is very promising to get much higher photodegradation efficiency by optimizing and integrating these parameters. These effects can be much higher in the case of more complex compounds such as DMMP and salicylic acid. Another possible reason for this is due to different surface area and using MeOH as a solvent. As discussed in section 3.1, oxidative electron transfer occurs exclusively through a surface-bound hydroxyl radical, $\{>TiOH^{\bullet}\}^{+}$ or equivalent trapped hole species. Degussa P25 powder is stoichiometric TiO_2. The TiOH radical might exist in the titanium oxide powder through sol-gel route thermal treated at low temperature. This may enhance the oxidation of chemical waste, especially in the case of non-aqueous solution.

Table III. Effects of various parameters on efficiency estimated from Phase I results

parameter	surface area	dye-sensitization	anatase/rutile	W doping	morphology
activity improvement	3	3.5	2	1.5	1.5

VII. IDENTIFICATION OF WORK FOR PHASE II PROGRAM

In order to fabricate both a very high efficient pilot-scale military reactor and a low cost large-scale commercial unit, the following technical objectives will be met in the Phase II research:

1) Systematic investigation of the processing conditions to further improve efficiency,

2) Optimizing factors, such as specific surface area, pore size, surface states, crystallographic phase, doping and dye-sensitized effects, on efficiency of the reactors,

3) Scaling up the pilot plant production of TiO_2 materials by the sol-gel process,

4. Designing and fabricating a pilot scale unit of multi-stage reactor with a flow rate of 1 gal/min. or greater with relatively low cost to be field tested with the Army,

5. Designing and fabricating a very high efficient unit with moderate cost,

6. Designing a multi-functional reactor for chemical waste treatment, hydrogen generator and also solar cell.

During Phase II, we also plan for commercialization of the photodegradation unit through our own effort or by joint venture with another company. Field tests other than Army will also be performed with some potential commercial users such as pesticide manufacturers, chemical and paper making plants. A business plan will be prepared in seeking Phase III fundings for eventual commercialization.

The main objectives in Phase II research are two-fold: 1) systematic study and optimization of factors to get highest efficiency and 2) convert this technique to military and civilian applications. The application includes two parts: a high grade reactor for military used chemical treatment and water purification system and a low cost commercial reactor for chemical waste treatment.

In Phase I, the feasibility of fabricating a high efficiency photochemical reactor by sol-gel route was successfully demonstrated. It was found that the efficiency of photochemical reactor for degradation of toxic and hazardous chemical substances is dependent on several factors: 1) Specific surface area of TiO_2 powder, 2) Surface state and morphologies of TiO_2, 3) Crystallographic phase of TiO_2 , 4) Doping effect, and 5) Dye-sensitization. The approach to make high efficient reactor has been identified in Phase I study. 10 times higher activity comparing to widely used Degussa P25 TiO_2 powder has been demonstrated in a short six-month effort. The reactor can be very high efficient with moderate cost or high efficient with low cost. Several technologies used in Phase I project offers the opportunity for photocatalytic (use powder) and photoelectrochemical (use cell structure) applications of chemical waste treatment. There are two reasons to use cell structure; one is to store solar energy for utilization at night; and secondary, since in the absence of O_2 or other electron acceptors, the rate of oxidation of chemical waste decreases dramatically, a cell structure can provide enough electron exchange between active surface and promote the reaction.

In Phase I study, TiO_2 powder with very high specific surface area was obtained.

Increasing specific surface area will decrease the particle size. In the case of small particle size, the band bending is small and charge separation occurs via diffusion. When the particle size decreases down to about 50 Å, quantum size effect should be taken into account. It is feasible to obtain quantum yields for photoredox processes approaching unity. Although the band gap of TiO_2 will be increased and surface states can not be ignored, the photocatalytic efficiency can still be expected to increase significantly.

Therefore, in Phase II program, investigation of effects of specific surface area, morphologies and surface states of the powder should be enhanced. The improvement of efficiency of the photocatalytic reactor can be obtained via several routes: transition element doping, increasing specific surface area, using dye-sensitized TiO_2, et al. All these factors count for certain improvement of efficiency. Optimization and integration of all the factors to reach the highest photochemical efficiency is another objective of Phase II program. We will investigate the process in detail and identify the most proper processing conditions to fabricate high efficient photoreactors.

In Phase I research, improvement of photochemical efficiency by using Ru dye-sensitized TiO_2 powder has been proven. Although the result shows about 3.5 times increase in the efficiency, but according to the works that has been done by Grätzel et.al. on solar cell, the increase in photochemical efficiency should be much higher, especially in the visible light region. Therefore, much more improvement can be expected in the Phase II study. Besides, the cost of ruthenium dye is relatively high at this stage. In Phase II project, we plan to investigate low-cost dyes, such as porphyrins and $Fe(CN)_6^{4-}$. Even though the improvement could be lower, by integrating with other factors and counting cost/performance issue, low-cost dyes should be able to use on some applications.

The efficiency of the reactor can be improved by increasing photoreactivity of TiO_2 semiconductor or by increasing quantity of TiO_2 semiconductor. However, latter is limited by decreasing of light penetration. This problem can be solved by using simi-transparent bulk TiO_2 aerogel, which can provide better light transmittance. TiO_2-SiO_2 aerogel will be another alternative to provide better light transmittance.

As shown in the results of Phase I project, bulk aerogels and aero-ormocers can be obtained using supercritical drying, which show the highest specific surface area and highest degradation rate of toxic chemicals. Furthermore, semi-transparency of the gels is helpful to improve the utilization of the sunlight. It can be expected that very high efficient reactor with moderate cost can be achieved using these materials. If reactor is constructed as a solar cell, electron transfer between circuit and electrodes will maintain high efficiency of the reactor even when the absence of O_2 and other electron acceptors happened. Besides, electricity can be stored in rechargeable batteries for night use to improve efficiency of the unit. TiO_2 has also been applied

for the destruction of microganisms such as bacteria and viruses. Therefore, it is possible to build portable water cleaners for mission or battleground use.

In Phase I research, several other techniques such as aerosol and drying the sol-gel powders using heating gun (blower). These techniques can prepare high surface area powders with relatively low cost. Results are somewhat compatible to that from aerogel route. These powders will also be prepared in the Phase II and paste as thick films on electrodes for the applications on the low-cost commercial photoelectrochemical reactor. The designing, efficiency study, and the operation conditions of this reactor can be used for the fabricating reactors with higher efficiency by using aerogel materials.

After the high efficient TiO_2 materials have been achieved and scaling up to a pilot production, then the reactors can also be scaling up to a pilot plant stage. A pilot scale unit with flow rate of approximately 1 gal/min or greater can be constructed and field tested to demonstrate efficient solar photocatalytic degradation of interest to the Army. Finally, the production cost will be estimated, a business plan will be developed and capital for Phase III commercialization will be sought.

VIII. REFERENCE

1. M. R. Hoffmann, S. T. Martin, W. Choi, and D. W. Bahnemann, Chem. Rev., 95 (1995) 69
2. J. Papp, S. Soled, K. Dwight, and A. Wold, Chem. Mater., 6 (1994)496
3. O'Regan, B., Moser, J., Anderson, M., and Gratzel, M., Nature 353(1991)771
4. J. Papp, S. Soled, K. Dwight, and A. Wold, Chem. Mater., 6 (1994)496
5. M.S. Ahmed and Y.A. Attia, J. of Nor-cryst. Solids, 186 (1995)402
6. A. Hagfeldt and M. Creatzel, Chem. Rev., 95 (1995)49
7. L.E. Brus, J. Phys. Chem., 90(1986)2555
8. S.T. Martin, H. Herrmannn and M..R. Hoffmann, Trans. Faraday Soc. 90 (1994)3315-3330
9. A. Hagfeldt and M. Crätzel, Chem. Rev., 95 (1995)49
10. R.P. Bickley, T. Gonzalez, and R.J.D. Tilley, J. Solid State Chem. 92 (1991)178
11. Lee, W., Gao, Y-M., Dwight, K., and Wold, A., Mater. Res. Bull, 27(1992)685
12. Matthews, R.W., Sol. Energy, 38(1987)405
13. Wang, C-M., Heller, A, and Gericher, H., J. Am. Chem. Soc., 114(1992)5230
14. Papp, J., Soled, S., Dwight, K., and Wold, A., Chem. Mater., 6(1994)496
15. Yoko, T., Kamiya, A., and Sakka, S., J. Electrochem. Soc., 138(1991)2279
16. O'Regan, B., Moser, J., Anderson, M., and Gratzel, M., Nature 353(1991)771
17.. K. Kalyanasundaram, and M. Grätzel, J. Phys. Chem. 91(1987)2342
18. E. Vrachnou, N. Vlachopoulos and M. Grätzel, J. Chem. Soc. Che,. Commun. 1987, 868
19. H. Scholze, J. Non-Cryst. Solids, 73(1985) 669-680
20. G.L. Wilkes and H. Huang, Polym. prepr. (Am. Chem. Soc., Polym. Chem.) 26 (1985) 300
21. G. Philipp and H. Schmidt, J Non-Cryst. Solids 63(9184) 283
22. G.L. Wilkes, H. Huang, Polym. Prepr. (Am.Chem.Soc., Div.Polym. Chem.) 26 (1985) 300
23. Y.J. Chung, S-J. Ting and J.D. Mackenzie, Mater.Res. Soc. Symp. Proc., 180 (1990)981
24. Y. Hu and J.D. Mackenzie, Mater.Res. Soc. Symp. Proc., Vol.271, (1992) pp 681
25. Jahn, W., Y. Hu and J.D. Mackenzie, in press.
26. C. Kormann, D.W. Bahnemann, and M.R. Hoffmannm Environ. Sci. Technol. 25(1991)494
27. G. Dagan and M. Tomkiewicz, Non-crystalline Solids, 175(1994)294
28. G. Garlson, D. Levis, K. McKinkey, and T. Tillotson, J. Non-cryst. Solids, 186 (1995)372